

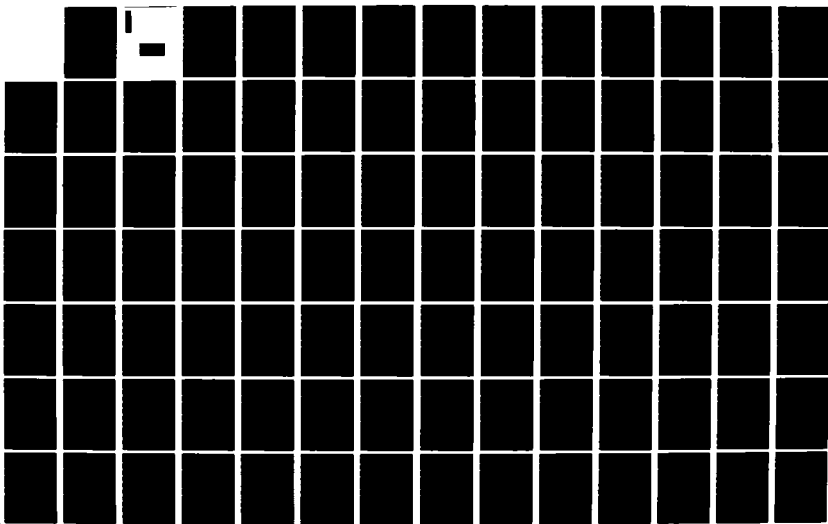
AD-A124 767

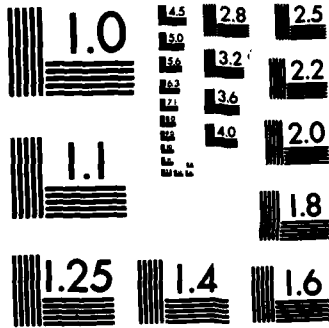
INVESTIGATION OF BINARY ERROR PROBABILITY FOR AN
INTEGRATE-AND-DUMP RECEI. (U) AIR FORCE INST OF TECH
WRIGHT-PATTERSON AFB OH SCHOOL OF ENGI. B T MELUSEN
DEC 82 AFIT/GE/EE/82D-49 .F/G 17/2

1/2

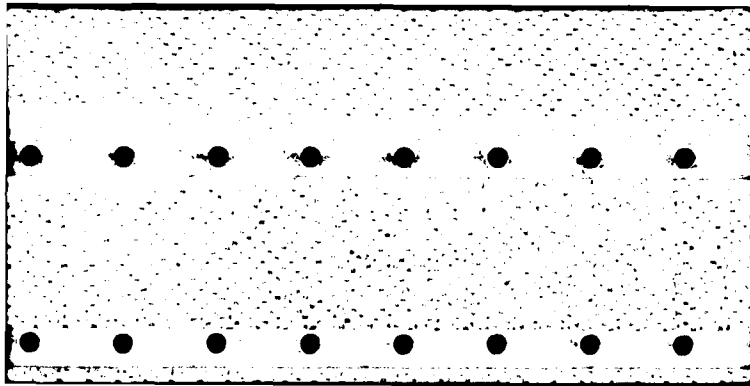
UNCLASSIFIED

NL





MICROCOPY RESOLUTION TEST CHART
NATIONAL BUREAU OF STANDARDS-1963-A



AFIT/GE/EE/82D-49

①

INVESTIGATION OF BINARY ERROR PROBABILITY
FOR AN INTEGRATE-AND-DUMP RECEIVER
AS OUTPUT QUANTIZATION INCREASES

AFIT/GE/EE/82D-49

Bruce T. Melusen
Captain USAF

DTIC
ELECTE
S FEB 22 1983 D

A

Approved for Public Release; Distribution Unlimited

AFIT/GE/EE/82D-49

INVESTIGATION OF BINARY ERROR PROBABILITY
FOR AN INTEGRATE-AND-DUMP RECEIVER
AS OUTPUT QUANTIZATION INCREASES

THESIS

Presented to the Faculty of the School of Engineering
of the Air Force Institute of Technology

Air Training Command
in Partial Fulfillment of the
Requirements for the Degree of
Master of Science

by

Bruce T. Melusen, B.S., M.B.A.

Captain

USAF

December 1982

Approved for Public Release; Distribution Unlimited

Preface

This topic was suggested by Lieutenant Colonel Ronald Carpinella because there are few published results that examine binary error probability for integrate-and-dump receivers. As fiber optic communications systems become more widely used, information concerning error probability as a function of output quantization will be of practical importance.

I am deeply indebted to the members of my advisory committee for their enthusiastic support, spirited interest and helpful suggestions. I especially want to thank Lieutenant Colonel Carpinella and Major Kenneth Castor, whose guidance has molded my formal course work and this research effort into a complete and truly outstanding educational experience. Their technical expertise and valued friendship will be long remembered.

Finally, and most importantly, to my wife, Deborah, I wish to express my deepest love and appreciation for her continued patience, understanding, assistance, and cooperation throughout the entire program.

Bruce T. Melusen

Accession For	
NTIS GRA&I	<input checked="" type="checkbox"/>
DTIC TAB	<input type="checkbox"/>
Unannounced	<input type="checkbox"/>
Justification	
Distribution/	
Availability Codes	
Avail. and/or	
Special	

A



Contents

	<u>Page</u>
Preface	ii
List of Figures	v
List of Tables	vii
List of Symbols	viii
Abstract	x
I. Introduction	1
II. Background	4
Optical Communication System Model	4
Integrate-and-Dump Receivers	4
Channel Characterization	6
Optimum Post-Detection Processing	7
Determining Probability of Error	9
Binary Input, Unquantized Binary Output	9
Summary	14
III. Increasing Output Quantization	17
Introduction	17
Channel Characterization	17
Post-Detection Processing	22
Probability of Error	24
Summary	25
IV. Cutoff Rate Analysis	27
Introduction	27
Cutoff Rate Development	27
Probability of Error Bound	28
Summary	29
V. Avalanche Detector with Output Quantization	31
Introduction	31
Channel Characterization	32
Post-Detection Processing	37
Probability of Error	38
Summary	38

Contents

	<u>Page</u>
VI. Conclusions	41
General Information	41
Ideal Detector, Quantized Output	43
Cutoff Rate Analysis	46
Avalanche Detector, Quantized Output	46
Topics for Future Research	50
Bibliography	51
Appendix A: Computer Programs	53
Appendix B: Data	65
Vita	90

List of Figures

<u>Figure</u>		<u>Page</u>
1	Optical Communication System Block Diagram . .	2
2	Integrate-and-Dump Receiver Block Diagram . .	5
3	Typical Binary Channel	6
4	Binary Input, Unquantized Output System . . .	9
5	Channel Characterization for $J = 2$	19
6	Quantized Output Post-Detection Processor . .	23
7	Ideal Detector, Probability of Error Flowchart	26
8	Avalanche Detector System Block Diagram . . .	32
9	Avalanche Detector, Probability of Error Flowchart	40
10	Probability of Error vs Quantizations for Ideal Detector (μ_0 constant : μ_1 varying) .	44
11	Probability of Error vs Quantizations for Ideal Detector (μ_0, μ_1 varying) :	45
12	Probability of Error vs Symmetric Cutoff Rate for Ideal Detector	47
13	Probability of Error vs Symmetric Cutoff Rate for Avalanche Detector	48
14	Probability of Error vs Quantizations for Avalanche Detector	49
15	Ideal Detector, Quantized Output Program Listing	54
16	Ideal Detector, Quantized Output Program Sample Output	56
17	Cutoff Rate Calculations Program Listing . . .	58
18	Cutoff Rate Calculations Program Sample Output	59
19	Avalanche Detector, Quantized Output Program Listing	61

Figure

Page

20	Avalanche Detector, Quantized Output Program	
	Sample Output	64

List of Tables

<u>Table</u>		<u>Page</u>
I	Probability of Error - Unquantized Output . .	16
II	Ideal Detector, Quantized Output	66
III	Symmetric Cutoff Rate for Ideal Detector . .	76
IV	Avalanche Detector, Quantized Output	78
V	Symmetric Cutoff Rate for Avalanche Detector	84

List of Symbols

<u>Symbol</u>	<u>Definition</u>
A_0	Detectors active surface area
C_R	Constant used in cutoff rate probability of error bound
D_i	Decide i
DMC	Discrete memoryless channel
g_i	Random gain factor for avalanche detector
hf_0	Energy of a photon
J	Quantizations - number of segment in T seconds
k	Ratio of hole ionization coefficient to electron ionization coefficient for avalanche detector
L	Number of bits encoded in cutoff rate probability of error bound
L_0	Threshold for the number of bits in the channel output required to be one to decide message one
M_i	Message i
MAP	Maximum a posteriori
N	Code constraint length in cutoff rate probability of error bound
$N(T)$	Number of counts in time period T
N_0	Threshold for the number of counts to decide message one
P_0	Probability channel output is zero given zero is input .
P_1	Probability channel output is one given one is input
$P_{n,n+r}$	Probability that $n+r$ counts are output from an avalanche detector given n counts are input
$P(E)$	Probability of error for the system
$Pr\{X\}$	Probability of X occurring

<u>Symbol</u>	<u>Definition</u>
$\Pr\{X Y\}$	Probability of X given Y
R_0	Cutoff rate
\tilde{R}_0	Symmetric cutoff rate
T	Time period for received signal
$\underline{U}_d(\underline{r}, t)$	Spatial and time varying optical field
μ_i	Average number of counts detected for message i
i	Factorial
$\lambda(t)$	Rate function
η	Detectors quantum efficiency
$[X]$	Largest integer less than X
$\lceil X \rceil$	Smallest integer greater than X

Abstract

→ The binary error probability for integrate-and-dump receivers is developed. The combination of the optical modulator, optical channel, and optical detector is characterized as a discrete memoryless channel (DMC). Maximum a posteriori (MAP) decision criteria are developed to enable optimal post-detection processing. The effect of quantizing the output is addressed for both ideal unity gain detector and avalanche detector optical systems. Multilevel Amplitude Keying is used to calculate specific probability of error values, and the channel cutoff rate is used to investigate probability of error bounds. ←

INVESTIGATION OF BINARY ERROR PROBABILITY
FOR AN INTEGRATE-AND-DUMP RECEIVER
AS OUTPUT QUANTIZATION INCREASES

·I Introduction

↓

This thesis effort focuses on direct detection optical communications systems which use receivers classified as photon counters, or integrate-and-dump receivers. These systems determine the received message estimate based upon the number of photons, or counts, accumulated in the specified reception time period, T . Figure 1 shows a typical block diagram of an optical communication system. X

This report centers on the examination of the optical channel, the optical detector, and the post-detection processor, or decision maker. The optical channel and detector are characterized, or modeled, and the post-detection processing is then optimized for the channel model to provide minimum probability of error for the system as a unit. The channel and detector are analyzed together and are modeled as a discrete memoryless channel (DMC) with characteristic crossover or transition probabilities. Using the channel model, the optimum post-detection processor is developed using maximum a posteriori (MAP) decision criteria and the resulting system is evaluated by determining the probability

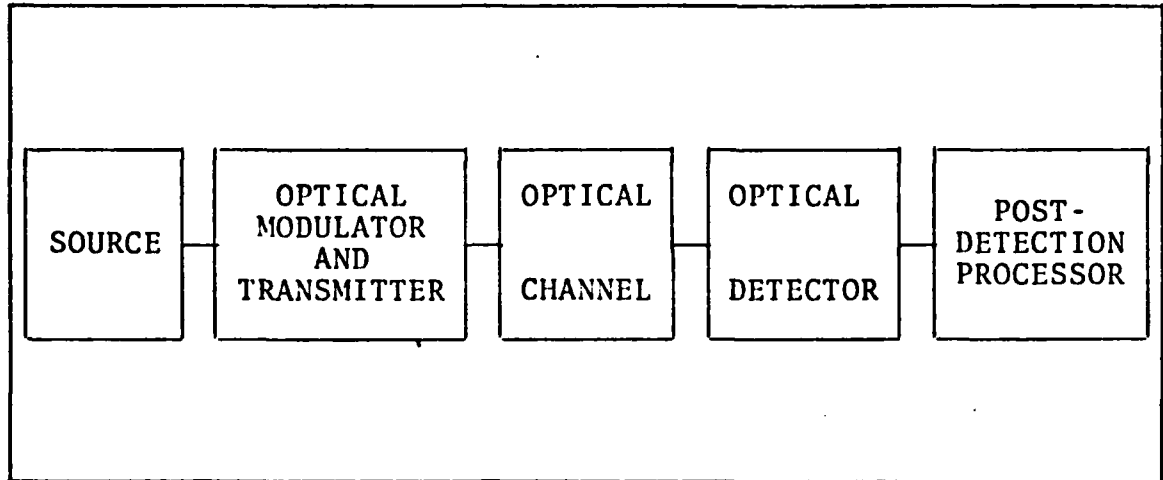


Figure 1. Optical Communication System Block Diagram

of error. The effect of quantizing the output of the detector, or dividing the time period T into smaller segments, is examined.

Throughout this work, a wideband direct detection receiver has been assumed to allow the signals to be viewed as point processes. This assumption essentially limits all disturbances to those associated with the conversion of the optical field to photons (Ref 2:113). A binary signal input field is assumed, however, the procedures used are easily generalized to an M -ary input field.

The concepts used to analyze the basic optical communication system of interest are developed in Chapter II. The general procedure used to characterize the channel/detector combination is presented, and the selection method for the optimum post-detection processor for unquantized output is examined. Chapter III introduces the idea of quantized

output and applies the concepts developed in Chapter II to communications systems employing increasingly finer output quantization. The cutoff rate approach to communications systems is presented in Chapter IV. The meaning of the cutoff rate is examined, and probability of error bounds are presented. Chapter V introduces a random gain factor to the output of the optical detector, modeling the effect of including an avalanche photodiode in the optical detection system. The effect of quantizing the output of the avalanche detector is examined by calculating probability of error information. The final chapter summarizes the major results of this research and discusses areas open for future research.

II Background

Optical Communication System Model

A typical optical communication system is shown in Figure 1. Some type of information is to be transmitted from a source to a distant destination by propagation of a modulated light signal. The information signal will vary a specific property of the transmitted light such as amplitude, frequency, or phase. The optical field detected at the receiver depends directly on the field that was transmitted, the effects introduced by the channel, and background radiation. The function of the receiver is to process the received optical field so as to reproduce an accurate estimate of the information signal.

Integrate-and-Dump Receivers

The development of the theory applicable to direct detection receivers has been well documented (Refs 2, 6, 8). Given a field incident on the detector surface, $\underline{\mathcal{E}}_d(\underline{r}, t)$, the rate function, $\lambda(t)$, is defined as:

$$\lambda(t) = (\eta/hf_0) \int_{A_0} |\underline{\mathcal{E}}_d(\underline{r}, t)|^2 d\underline{r} \quad (1)$$

where

- η = detectors quantum efficiency
- hf_0 = energy of a photon
- A_0 = detectors active surface area

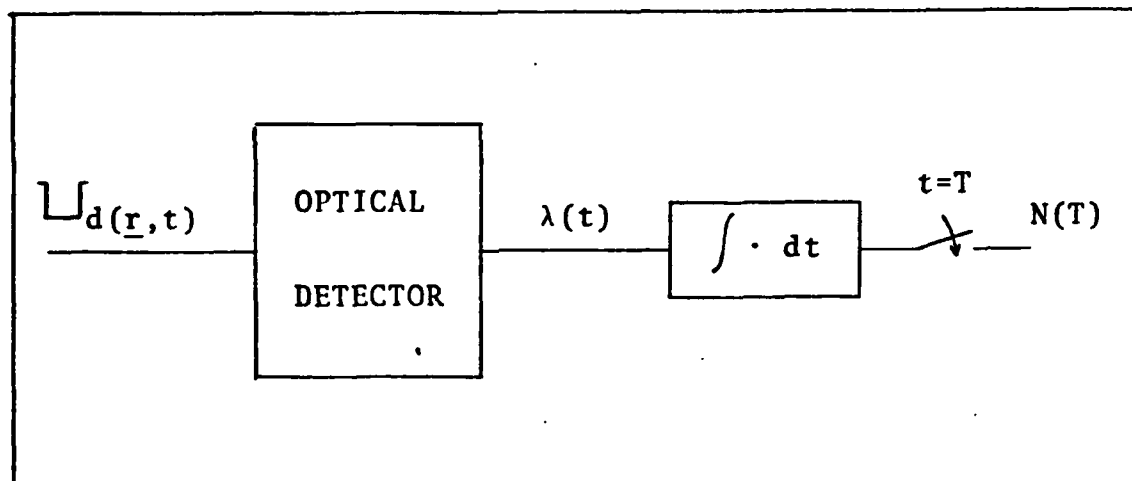


Figure 2. Integrate-and-Dump Receiver Block Diagram

This rate function, $\lambda(t)$, gives the number of photons incident on the detector, per time period, for a given optical field. In optical communications systems which use photon sensitive detectors, the emission of the photoelectrons corresponds to a point process obeying Poisson statistics (Refs 1, 18).

The block diagram of an integrate-and-dump receiver shown in Figure 2 gives an overall view of how the counting of photons is implemented. By integrating the output of the detector, the rate function $\lambda(t)$, over the time period T , a total number of counts for T , $N(T)$, is obtained. This number, $N(T)$, reflects the number of photons emitted by the detector in time T . Thus, as different optical fields, $U_i(\underline{r}, t)$, will be associated with each of the i possible source messages, there will also be different rates, $\lambda_i(t)$, and counts, $N_i(T)$, associated with each source message.

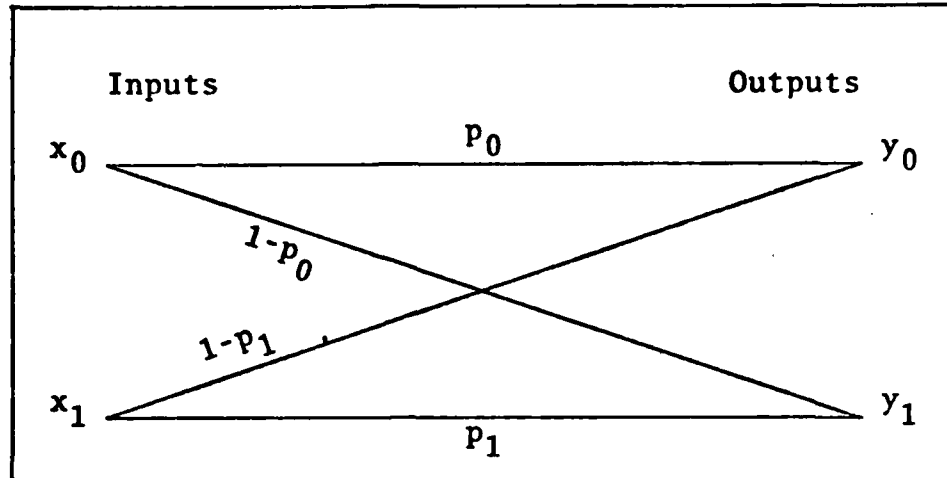


Figure 3. Typical Binary Channel

Channel Characterization

As demonstrated by Snyder and Rhodes (Ref 17:327), the combination of the optical modulator, optical channel, and the optical detector, when considered as a unit, forms a discrete channel. For the purpose of this study, the channel will be assumed to be memoryless, that is, the channel output at any given time is a function of the channel input at that time and is independent of all previous inputs. A discrete memoryless channel (DMC) can be completely specified by the set of conditional probabilities which relate the probability of each output to the various inputs (Ref 7:6).

The assumption of a binary input signal set leads to the use of a binary input channel shown in Figure 3. By combining the modulator, channel, and detector to form a DMC and determining the probabilities p_0 and p_1 of Figure 3, it becomes possible to determine the optimum post-detection

processing that will be required to produce minimum probability of error estimates.

Optimum Post-Detection Processing

The optimum post-detection processing is that processing of the channel output required to provide an estimate of the input information signal while maintaining the system probability of error at a minimum. Essentially, the post-detection processor is a decision maker that determines what the input information signal was, based on the output of the channel.

The optimum post-detection processing reduces to simple photon counting for the following cases:

- 1 - When $\lambda_i(t)$ is a constant for t within the specified time period of interest, $t \in [0, T]$;
- 2 - When $\lambda_i(t)$ is the same for all signals, but the signals are spatially separated; or,
- 3 - When $\lambda_i(t)$ are nonoverlapping, or orthogonal, in time.

The first case is commonly called Multilevel Amplitude Keying, while the third case is Pulse Position Modulation (Ref 2:171). This report will give examples for Multilevel Amplitude Keying. By assuming Multilevel Amplitude Keying, the dark current, which is a homogeneous Poisson process with rate λ_D , can be included within the rates λ_i because the dark current will have the same effect on any of the received signals. That is, the rate λ_D , when integrated

over time period T, will add a certain number of counts independent of which source message was transmitted.

To ensure optimum post-detection processing, that is, minimum probability of error for the system, the maximum a posteriori (MAP) decision criterion will be used. The MAP decision criterion states that given an observation, Y, select decision one if M_1 is more probable than M_0 to have been the input information signal which produced Y (Ref 13:42). Mathematically, the decision criterion can be written:

$$\frac{\Pr\{M_1|Y\}}{\Pr\{M_0|Y\}} \begin{matrix} > \\ < \end{matrix} \begin{matrix} D_1 \\ D_0 \end{matrix} \quad 1 \quad (2)$$

By using Bayes rule, Eq (2) can be rewritten as:

$$\frac{\Pr\{Y|M_1\}}{\Pr\{Y|M_0\}} \begin{matrix} > \\ < \end{matrix} \begin{matrix} D_1 \\ D_0 \end{matrix} \frac{\Pr\{M_0\}}{\Pr\{M_1\}} \quad (3)$$

This introduces the concept of decision regions. Whenever the left-hand side of Eq (3), commonly called the likelihood ratio, is greater than the threshold, given by the right-hand side of Eq (3), the decision is made that M_1 was the information transmitted. Thus, the threshold divides space into two decision regions: one where the likelihood ratio is greater than the threshold and another where it is less.

Returning to the ideal photon detector, the optimum post-detection processor will decide that information message one was transmitted whenever the probability that

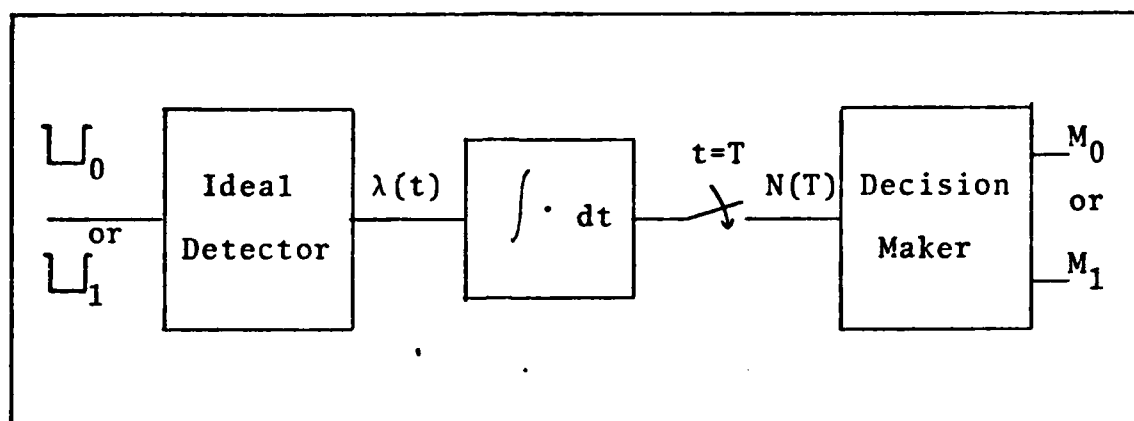


Figure 4. Binary Input, Unquantized Output System

the number of counts obtained, $N(T)$, was more likely given message one than message zero.

Determining Probability of Error

Once the decision regions have been determined, the system probability of error can be calculated. The total probability of error is simply the probability of deciding message zero when message one was sent plus the probability of deciding message one when message zero was sent. Mathematically:

$$P(E) = \Pr\{D_0, M_1\} + \Pr\{D_1, M_0\} \quad (4)$$

and, using conditional probabilities:

$$P(E) = \Pr\{D_0|M_1\}\Pr\{M_1\} + \Pr\{D_1|M_0\}\Pr\{M_0\} \quad (5)$$

Binary Input, Unquantized Binary Output

The system shown in Figure 4 is a binary input, unquantized output optical communication system receiver. A

binary input alphabet of M_0 and M_1 produce optical fields \mathcal{L}_0 and \mathcal{L}_1 incident to the ideal detector. The output of the ideal detector is the rate function, either $\lambda_0(t)$ or $\lambda_1(t)$. The rate function is integrated over the time period T , producing a count, $N(T)$. This count, or the number of photoelectrons produced, is input to the decision maker, which using the MAP decision criterion, will determine which message, M_0 or M_1 , was transmitted.

The characterization of the channel is the first step to be examined. As previously discussed, for an ideal detector, the count $N(T)$ is distributed as a Poisson process. Thus:

$$\Pr\{N(T) = n\} = \frac{\mu^n e^{-\mu}}{n!} \quad (6)$$

where

$$\mu = \int_0^T \lambda(\alpha) d\alpha \quad (7)$$

Equation (7) determines the parameter μ , the average number of counts in time T .

For the unquantized detector output, the parameter μ is determined by integrating $\lambda(t)$ over the time period T . Since each input signal, M_0 and M_1 , will have a corresponding rate, $\lambda_0(t)$ and $\lambda_1(t)$, two μ parameters, μ_0 and μ_1 , will be defined. Applying these values for μ into Eq (6) gives:

$$\Pr\{N(T) = n | M_0\} = \frac{\mu_0^n e^{-\mu_0}}{n!} \quad (8)$$

and

$$\Pr\{N(T) = n | M_1\} = \frac{\mu_1^n e^{-\mu_1}}{n!} \quad (9)$$

Now that the probability of receiving $N(T) = n$ counts is known for any n , given either M_0 or M_1 was transmitted, Eq (3) can be used to define the decision regions. Applying the MAP decision rule of Eq (3) to the case of unquantized outputs given by Eqs (8) and (9) results in:

$$\frac{\frac{\mu_1^n e^{-\mu_1}}{n!}}{\frac{\mu_0^n e^{-\mu_0}}{n!}} \begin{matrix} D_1 \\ > \\ < \\ D_0 \end{matrix} \frac{\Pr\{M_0\}}{\Pr\{M_1\}} \quad (10)$$

Since n , the number of counts, is the variable of interest, the decision regions should be defined as functions of n . To determine the value for n of interest, Eq (10) is manipulated as follows:

$$\left(\frac{\mu_1^n e^{-\mu_1}}{n!}\right) \left(\frac{n!}{\mu_0^n e^{-\mu_0}}\right) \begin{matrix} D_1 \\ > \\ < \\ D_0 \end{matrix} \frac{\Pr\{M_0\}}{\Pr\{M_1\}} \quad (11)$$

$$\frac{\mu_1^n e^{-\mu_1}}{\mu_0^n e^{-\mu_0}} \begin{matrix} D_1 \\ > \\ < \\ D_0 \end{matrix} \frac{\Pr\{M_0\}}{\Pr\{M_1\}} \quad (12)$$

$$\left(\frac{\mu_1}{\mu_0}\right)^n e^{-(\mu_1 - \mu_0)} \begin{matrix} D_1 \\ > \\ < \\ D_0 \end{matrix} \frac{\Pr\{M_0\}}{\Pr\{M_1\}} \quad (13)$$

$$\left(\frac{\mu_1}{\mu_0}\right)^n \begin{matrix} > D_1 \\ < D_0 \end{matrix} e^{(\mu_1 - \mu_0)} \left(\frac{\Pr\{M_0\}}{\Pr\{M_1\}}\right) \quad (14)$$

$$n \ln\left(\frac{\mu_1}{\mu_0}\right) \begin{matrix} > D_1 \\ < D_0 \end{matrix} (\mu_1 - \mu_0) + \ln\left(\frac{\Pr\{M_0\}}{\Pr\{M_1\}}\right) \quad (15)$$

$$n \begin{matrix} > D_1 \\ < D_0 \end{matrix} \frac{(\mu_1 - \mu_0) + \ln\left(\frac{\Pr\{M_0\}}{\Pr\{M_1\}}\right)}{\ln\left(\frac{\mu_1}{\mu_0}\right)} \quad (16)$$

for all $\mu_1 > \mu_0$. Thus, Eq (16) gives the decision regions based on n , the number of counts. The threshold value is given by the right-hand side of Eq (16):

$$N_0 = \frac{(\mu_1 - \mu_0) + \ln\left(\frac{\Pr\{M_0\}}{\Pr\{M_1\}}\right)}{\ln\left(\frac{\mu_1}{\mu_0}\right)} \quad (17)$$

If $N(T)$ is greater than N_0 , the decision is made that M_1 was transmitted. Alternatively, if $N(T)$ is less than N_0 , the decision is made that M_0 was transmitted.

The count, $N(T)$, will always be an integer value, while the threshold, N_0 , is continuous and may take on any value. For cases where N_0 is not an integer, the decision regions are defined by deciding M_0 for all $N(T)$ which take on integer values less than N_0 and deciding M_1 for all $N(T)$ which take on integer values greater than N_0 . If N_0 is an

integer value, the case of $N(T) = N_0$ must also be considered since the probability of $N(T) = N_0$ is no longer zero, as is the case when N_0 is not an integer. The question of which decision is to be made when on the boundary of the decision regions is answered as follows--Choose M_1 for β percent of the time when $N(T) = N_0$, where β is given by:

$$\beta = \frac{\alpha - \Pr\{N(T) > N_0 | M_0\}}{\Pr\{N(T) = N_0 | M_0\}} \quad (18)$$

and α is a parameter chosen by the user, satisfying:

$$\Pr\{N(T) > N_0 | M_0\} < \alpha < \Pr\{N(T) \geq N_0 | M_0\} \quad (19)$$

(Ref 2:125D-125I). While M_1 may be chosen arbitrarily when $N(T) = N_0$, the procedure outlined above allows the user to determine what performance, or probability of false alarm, is acceptable by varying the parameter α .

Thus, the optimum post-detection processor makes the decision between M_0 and M_1 by comparing the received count, $N(T)$, to the threshold value, N_0 , and choice of M_0 or M_1 depends on whether $N(T)$ is less than, greater than, or equal to N_0 .

The probability of error for the binary system is given by Eq (5). The prior probabilities of M_0 and M_1 are assumed to be known, and the probabilities of making an incorrect decision are given by:

$$\Pr\{D_1 | M_0\} = \Pr\{N(T) > N_0 | M_0\} \quad (20)$$

or

$$\Pr\{D_1|M_0\} = \sum_{n=[N_0]}^{\infty} \frac{\mu_0^n e^{-\mu_0}}{n!} \quad (21)$$

and

$$\Pr\{D_0|M_1\} = \Pr\{N(T) < N_0|M_1\} \quad (22)$$

or

$$\Pr\{D_0|M_1\} = \sum_{n=0}^{[N_0]} \frac{\mu_1^n e^{-\mu_1}}{n!} \quad (23)$$

Therefore, all of the terms of Eq (5) are known and the probability of error can be calculated.

Summary

The calculation of binary error probability for an integrate-and-dump receiver is accomplished in a straightforward manner. The first step is to characterize or model the channel. Then, using the channel model, the optimum post-detection processor for that channel must be determined. Once these steps have been completed, the probability of error is a direct result.

For the unquantized output case, the MAP decision rule is determined directly from the known values for the prior probabilities of M_0 and M_1 and the average counts received for each message, μ_0 and μ_1 . Table I lists calculated values of the probability of error for various values of

prior probabilities and average counts per message. Appendix A, Figure 15 is a listing of the BASIC language computer program used to calculate the data. Appendix B, Table II is a listing of calculated data for both quantized and unquantized output, ideal detector systems.

TABLE I
Probability of Error - Unquantized Output

<u>Pr{M₀}</u>	<u>Pr{M₁}</u>	<u>μ₀</u>	<u>μ₁</u>	<u>N₀</u>	<u>P(E)</u>
0.1	0.9	1	4	0.58	0.0797
0.1	0.9	1	5	1.12	0.0628
0.3	0.7	1	4	1.55	0.1434
0.3	0.7	1	5	1.96	0.1076
0.5	0.5	1	4	2.16	0.1592
0.5	0.5	1	5	2.49	0.1025
0.7	0.3	1	4	2.78	0.1276
0.7	0.3	1	5	3.01	0.0928
0.9	0.1	1	4	3.74	0.0604
0.9	0.1	1	5	3.85	0.0436

III Increasing Output Quantization

Introduction

Having already developed the procedure for determining the optimum post-detection processing scheme and the resultant probability of error for unquantized output, ideal detector receivers, this section introduces output quantization into the model. The characterization of the channel will be re-examined, the optimum post-detection processor will be redefined, and the resulting probability of error will be calculated for varying levels of output quantization.

Channel Characterization

For the unquantized output communication system, the channel model resulted in a count of photoelectrons, $N(T)$. As output quantization is introduced, the time period T is divided into shorter length segments. By doing this, the count $N(T)$ is also broken up into several counts, one count for each segment in T . For example, if T is segmented into two segments, each of $(T/2)$ duration, then there will now be two counts associated with T , one for each $(T/2)$ time interval. In general, if T is segmented into J intervals, each of duration (T/J) , then there will be J individual counts to be considered in the decision process. These J individual counts will be symbolized by N_i , for $i = 1$ to J , and J is the quantization level of the output. It is

important to note that the unquantized system is obtained by setting J equal to one.

By quantizing the output, the decision will now be based on J bits of information, the N_i counts, rather than the single count, $N(T)$. By using a MAP decision rule on each count, N_i , and deciding M_0 or M_1 for each count, a J bit long string of zeros and ones can be developed. It is this J bit long string that will be the output of the channel and the input of the decision maker for deciding whether M_0 or M_1 was transmitted, and the optimum post-detection processor must make the decision with minimum probability of error.

The channel characterization for the quantized output system requires the determination of the transition probabilities associated with each of the 2^J possible channel outputs of J bit strings of zeros and ones. Figure 5 shows a possible channel characterization for $J = 2$.

As was the case for unquantized output, the N_i counts for $i = 1$ to J , obey Poisson statistics as given by Eq (6). Due to the quantization, however, Eq (7) is modified to:

$$\mu_{i,J,n} = \int_{nT/J}^{(n+1)T/J} \lambda_i(\alpha) d\alpha \quad \text{for } n=0 \text{ to } (J-1) \quad (24)$$

because $\lambda_i(t)$ is no longer integrated over the entire period T , but only for intervals of (T/J) duration. By assuming Multilevel Amplitude Keying, Eq (24) reduces to:

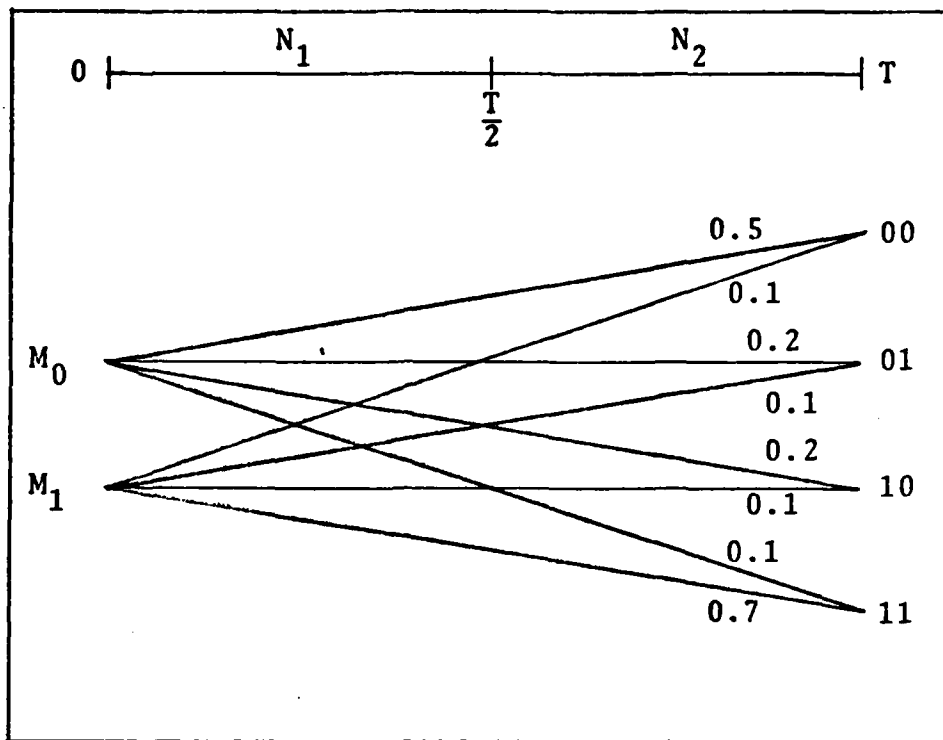


Figure 5. Channel Characterization for $J = 2$

$$\mu_{i,J} = \int_0^{(T/J)} \lambda_i(\alpha) d\alpha = \frac{\mu_i}{J} \quad (25)$$

Now, the MAP decision rule of Eq (3) can be applied to each of the J segments giving:

$$\frac{\Pr\{N_i = n | M_1\}}{\Pr\{N_i = n | M_0\}} \begin{matrix} > \\ < \\ > \end{matrix} \begin{matrix} D_1 \\ D_0 \\ D_0 \end{matrix} \frac{\Pr\{M_0\}}{\Pr\{M_1\}} \quad (26)$$

where

$$\Pr\{N_i = n | M_1\} = \frac{(\mu_1/J)^n e^{-(\mu_1/J)}}{n!} \quad (27)$$

and

$$\Pr\{N_i = n | M_0\} = \frac{(\mu_0/J)^n e^{-(\mu_0/J)}}{n!} \quad (28)$$

Substituting Eqs (27) and (28) into Eq (26) and simplifying, as was done previously in Eqs (11) through (16), the MAP decision rule for each of the J segments becomes:

$$n \begin{matrix} > D_1 \\ < D_0 \end{matrix} \frac{\frac{\mu_1 - \mu_0}{J} + \ln\left(\frac{\Pr\{M_0\}}{\Pr\{M_1\}}\right)}{\ln\left(\frac{\mu_1}{\mu_0}\right)} = N_{0,J} \quad (29)$$

Thus, for each of the J segments of T, if the count for a segment, N_i , is greater than the threshold, $N_{0,J}$, set the bit for that segment to zero. For $N_i = N_{0,J}$, the procedure discussed in Chapter II using Eq (18) is used to make the decision. Each count for the J segments is evaluated this way until a J bit long string of zeros and ones has been formed. This string then represents the output of the quantized channel.

To fully characterize the channel, the transition probabilities for each of the 2^J possible channel outputs are required. To determine the transition probabilities for the J bit long strings, the crossover probability for each of the J segments must be known. That is, the probability of setting a segment's bit to a one given M_0 was transmitted and the probability of setting a segment's bit to a zero given M_1 was transmitted must be determined. The procedure

to determine these bit transition probabilities is the same as was used to calculate the system probability of error in Chapter II. The results, similar to Eqs (21) and (23), are:

$$\Pr\{D_1|M_0\} = \sum_{n=\lfloor N_{0,J} \rfloor}^{\infty} \frac{\left(\frac{\mu_0}{J}\right)^n e^{-\left(\frac{\mu_0}{J}\right)}}{n!} = (1 - p_0) \quad (30)$$

and

$$\Pr\{D_0|M_1\} = \sum_{n=0}^{\lfloor N_{0,J} \rfloor} \frac{\left(\frac{\mu_1}{J}\right)^n e^{-\left(\frac{\mu_1}{J}\right)}}{n!} = (1 - p_1) \quad (31)$$

These determine the single bit transition probabilities. For an arbitrary J , the transition probabilities associated with a particular J bit long string are simple to calculate. The steps are as follows:

- 1 - Let the number of ones in the J bit string equal v , then the number of zeros in the string is $J - v$;
- 2 - To determine the transition probability of the particular string, given M_1 was transmitted:

$$\Pr\{(J \text{ bit string})|M_1\} = p_1^v (1 - p_1)^{J - v} \quad (32)$$

where $(1 - p_1)$ is given by Eq (31);

- 3 - To determine the transition probability of the particular string, given M_0 was transmitted:

$$\Pr\{(J \text{ bit string})|M_0\} = p_0^{J-v}(1 - p_0)^v \quad (33)$$

where $(1 - p_0)$ is given by Eq (30).

At this point, a model which fully characterizes the channel has been developed. The "hard decision" channel of the unquantized output system, where the number of inputs to the channel equals the number of channel outputs, has become a "soft decision" channel for the quantized output system, where there are a larger number of possible channel outputs than inputs. Massey (Ref 11) and Lee (Ref 10) show that probability of error criterion is applicable only for "hard decisions" and that a cutoff rate based criterion offers more guidance for "soft decision" system design. This topic is covered in Chapter IV. The next step to be covered for the quantized output system is how to determine what post-detection processing is required to produce optimum results.

Post-Detection Processing

Once the channel is characterized, the post-detection processor which will take the J bit string of zeros and ones output by the channel and determine whether M_0 or M_1 was transmitted with a minimum probability of error must be developed. Figure 6 is a block diagram of this type of decision maker.

To ensure minimum probability of error, the MAP decision criterion of Eq (3) will be used once again. For any J bit string of zeros and ones output by the channel,

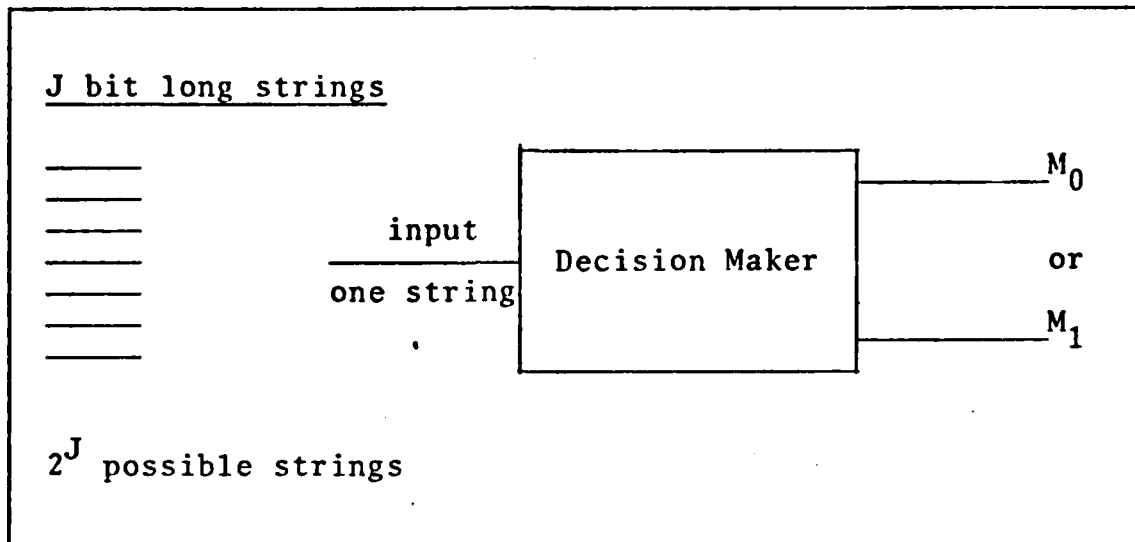


Figure 6. Quantized Output Post-Detection Processor

implementing the MAP decision rule of Eq (3) yields:

$$\frac{\Pr\{X_1 X_2 \dots X_J | M_1\}}{\Pr\{X_1 X_2 \dots X_J | M_0\}} \underset{D_0}{\overset{D_1}{>}} \frac{\Pr\{M_0\}}{\Pr\{M_1\}} \quad (34)$$

where $X_1 X_2 \dots X_J$ is the J bit long string of zeros and ones. Substituting Eqs (32) and (33) into Eq (34) results in:

$$\frac{p_1^v (1 - p_1)^{J - v}}{p_0^J - v (1 - p_0)^v} \underset{D_0}{\overset{D_1}{>}} \frac{\Pr\{M_0\}}{\Pr\{M_1\}} \quad (35)$$

where v is the number of ones in the J bit string. Similar to the steps taken to determine $N_{O,J}$ in Eq (29), Eq (35) can be simplified, yielding:

$$v \begin{matrix} D_1 \\ > \\ < \\ D_0 \end{matrix} \frac{\ln \left(\frac{\Pr\{M_0\}}{\Pr\{M_1\}} \right) - J \ln \left(\frac{1 - p_0}{p_0} \right)}{\ln \left(\frac{p_0 p_1}{(1 - p_0)(1 - p_1)} \right)} = L_0 \quad (36)$$

Thus, the decision maker of Figure 6 determines whether M_0 or M_1 was transmitted by deciding if v , the number of ones in the J bit string is greater than or less than L_0 . For all J bit strings where the number of ones is greater than the threshold, L_0 , M_1 is decided to have been transmitted. If the number of ones is less than L_0 , then M_0 is decided. For $v = L_0$, the procedure discussed previously in Chapter II using Eq (18) is used to make the decision.

Probability of Error

The system probability of error, $P(E)$, is again given by:

$$P(E) = \Pr\{D_1|M_0\}\Pr\{M_0\} + \Pr\{D_0|M_1\}\Pr\{M_1\} \quad (5)$$

For systems using quantized output, Eq (5) reduces to:

$$P(E) = \left[\sum_{v=0}^{\lfloor L_0 \rfloor} \binom{J}{v} p_1^v (1 - p_1)^{J - v} \right] \Pr\{M_1\} + \left[\sum_{v=\lceil L_0 \rceil}^J \binom{J}{v} p_0^v (1 - p_0)^{J - v} \right] \Pr\{M_0\} \quad (37)$$

where

$$\binom{J}{v} = \frac{J!}{v!(J-v)!} = \text{binomial coefficients} \quad (38)$$

Summary

As the output is quantized, the calculation of the probability of error becomes more complex. Following the methods used for unquantized systems, the channel is modeled and post-detection processing is developed to conform with the channel model. Given the prior probabilities and the count parameters for M_0 and M_1 , and the quantization level, J , the probability of error for the system can be calculated directly. Figure 7 shows a simple flowchart used to calculate probability of error. Appendix A, Figure 15 is a listing of the BASIC language computer program used to compute data. Appendix B, Table II lists calculated data for both quantized and unquantized output, ideal direct detection systems.

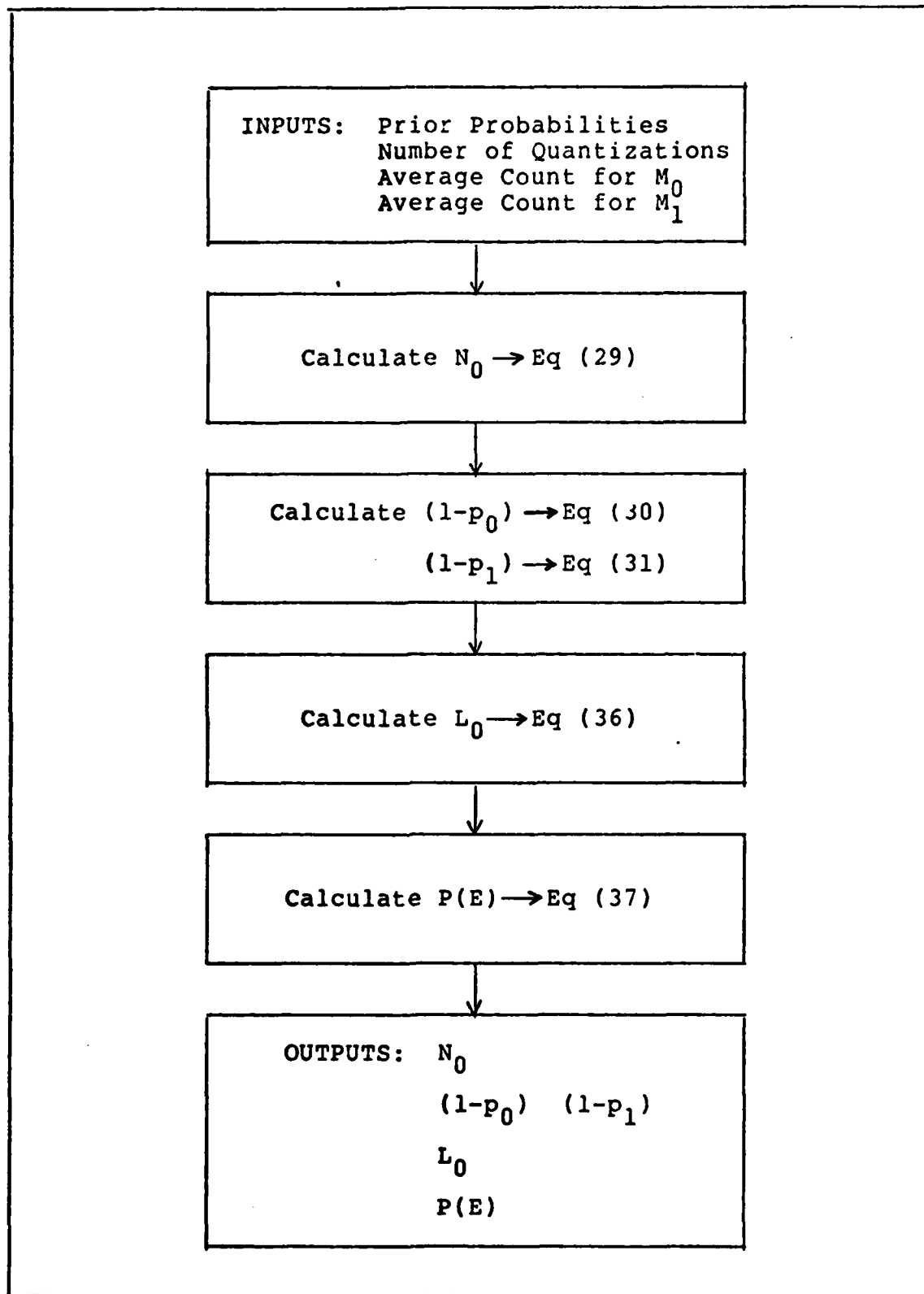


Figure 7. Ideal Detector, Probability of Error Flowchart

IV Cutoff Rate Analysis

Introduction

The design criterion for modulation systems in almost universal use is probability of error. While probability of error is meaningful for "hard decision" systems, where the number of outputs correspond exactly to the number of inputs, the meaning of error in a "soft decision" system, where the number of outputs is greater than the number of inputs, is rather nebulous. For this reason, another more meaningful design criterion would prove useful for "soft decision" communication systems.

Cutoff Rate Development

Wozencraft and Kennedy (Ref 25) were the first to suggest the use of the "cutoff rate," R_0 , as a design criterion for a discrete memoryless channel (DMC). The cutoff rate was chosen because it is the upper limit of code rates for which the average decoding computation per source digit is finite when sequential decoding is used (Ref 17:328). Massey (Ref 11) observed that R_0 gives more information about the DMC than the channel capacity because R_0 relates both a range of rates for reliable communication, as well as the necessary coding complexity to achieve a specific error probability.

As developed previously, a DMC of M inputs and Q outputs can be completely described by the transition

probabilities, $\Pr\{q|m\}$, the probability the channel output is q given the channel input is m . The cutoff rate, R_0 , is defined by using these transition probabilities as follows:

$$R_0 = -\log_2 \left\{ \min_{\substack{P \\ q=0}} \sum_{m=0}^{Q-1} \left[\sum_{m=0}^{M-1} p(m) \sqrt{\Pr\{q|m\}} \right]^2 \right\} \quad (39)$$

where p is a probability distribution for the M channel input signals. When p is the uniform distribution, the cutoff rate defined by Eq (39) is called the symmetric cutoff rate, \tilde{R}_0 , given by:

$$\tilde{R}_0 = \log_2 M - \log_2 \left\{ \frac{1}{M} \sum_{m=0}^{Q-1} \left[\sum_{m=0}^{M-1} \sqrt{\Pr\{q|m\}} \right]^2 \right\} \quad (40)$$

Additionally, $\tilde{R}_0 = R_0$ for the binary input case where the uniform distribution is always the minimizing distribution and in most other cases of practical interest where the modulation signal set and the demodulator decision regions are reasonably symmetric (Ref 10:438).

Probability of Error Bound

Wozencraft and Kennedy (Ref 25) showed that there is a block code of rate R and codeword length N such that the probability of error $P(E)$ is bounded by:

$$P(E) \leq 2^{-N(R_0 - R)} \quad \text{if } R < R_0 \quad (41)$$

For convolutional codes, Viterbi (Ref 22) has shown that the decoding error probability is upperbound as follows:

$$P(E) \leq c_R L 2^{-NR_0} \quad \text{if } R < R_0 \quad (42)$$

where

N = code constraint length

L = number of bits encoded

c_R = multiplying factor independent of N and L

R_0 = cutoff rate

Throughout this report, block codes have been used, thus Eq (41) applies. As stated previously, $\tilde{R}_0 = R_0$ for the binary input case, so Eq (41) can be rewritten:

$$P(E) \leq 2^{-N(\tilde{R}_0 - R)} \quad \text{if } R < \tilde{R}_0 \quad (43)$$

Examining Eq (43), it should be noted that the probability of error bound will become smaller as the symmetric cutoff rate increases. Additionally, the bound may be made arbitrarily small by increasing N , as long as the $R < \tilde{R}_0$ condition is satisfied.

Thus, a new decision criteria, based on cutoff rates for either block or convolutional codes can be developed. To decrease the probability of error bounds given by Eqs (41), (42) and (43), the cutoff rate should be maximized.

Summary

For systems that employ "hard decision" channels such as the unquantized output of an ideal unity gain detector discussed in Chapter II, the probability of error design criterion is quite meaningful. However, if a "soft

decision" channel is used, such as in the quantized output systems discussed in Chapter III, the probability of error is meaningless, and another criterion must be developed. The cutoff rate criterion has proven to be a very effective method for design of these "soft decision" channel systems.

The symmetric cutoff rate, \tilde{R}_0 , is calculated using the transition probabilities that characterize the channel model. This value for \tilde{R}_0 can then be used to determine an upper bound on the probability of error for the DMC given a specific code rate R .

Appendix A, Figure 17 is a listing of the BASIC language computer program used to calculate the symmetric cutoff rate, \tilde{R}_0 , for the various systems from Appendix B, Tables II and IV. Calculated values of \tilde{R}_0 are presented in Appendix B, Tables III and V, along with calculated $P(E)$ values for comparison.

V Avalanche Detector with Output Quantization

Introduction

Chapter III examined optical direct detection receivers assuming an ideal gain factor of one. This chapter assumes the receiver now uses an avalanche detector. Since the gain of an avalanche detector is random (Ref 15:161), its statistics will have an impact on system performance. To determine the impact that the random gain has, the probability of the number of output photoelectrons, given the number of photoelectrons input to the avalanche detector is required. While several authors have conceived differing values for the probability distribution of interest (Refs 4,14,16), the most complete development has been formulated by McIntyre (Ref 12). The probability distribution derived by McIntyre will be used in this section to provide the required information about the avalanche detector random gain. The probability is given by:

$$P_{n,n+r} = \frac{n}{[2\pi(n+r)(n+kr)r]^{\frac{1}{2}}} \left(1 - \frac{nX}{r}\right)^r \cdot \left(1 + \frac{n(1-k)X}{n+kr}\right)^{\frac{n+kr}{1-k}} \quad (44)$$

where

n = number of counts input to the avalanche detector

$n+r$ = number of counts output by the avalanche detector

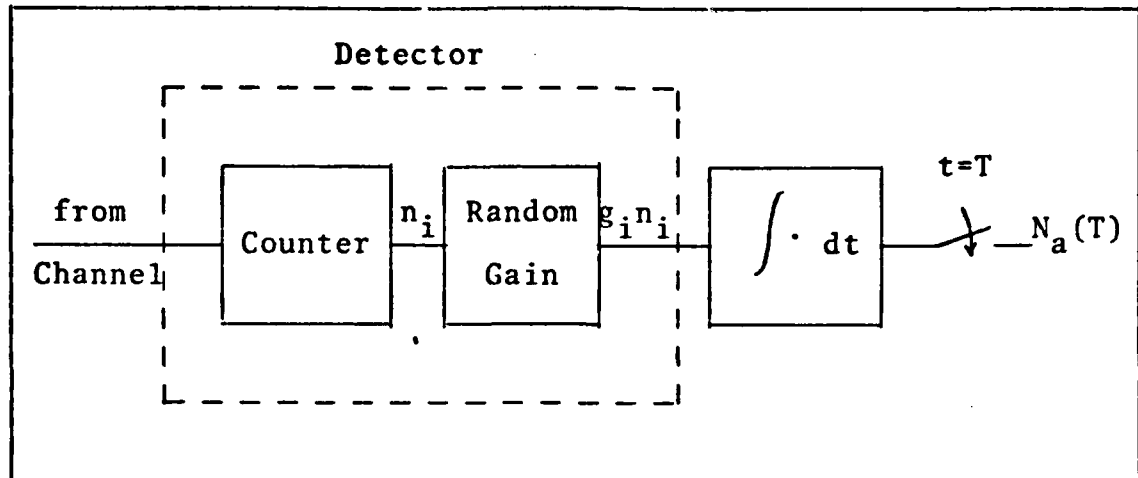


Figure 8. Avalanche Detector System Block Diagram

k = ratio of the hole ionization coefficient to the electron ionization coefficient for the avalanche detector

$$X = \frac{n + r - nM}{nM}$$

and M is the average gain of the avalanche detector.

By using the probability given by Eq (44) to modify the equations from Chapter III, the effect of introducing an avalanche detector into the optical communication system becomes a logical extension of the ideal unity gain detector previously examined.

Channel Characterization

The procedure used to model the channel for a communication system with an avalanche detector parallels closely to that used previously in Chapter III where unity gain was assumed. Figure 8 shows a block diagram of an avalanche detector system. Instead of each photon having a count of

one, a random value, g_i , must be multiplied by each count to determine the total count for time interval T . That is, while for the ideal unity gain detector, the total count was given by:

$$N(T) = \sum_i n_i \quad (45)$$

the inclusion of the avalanche detector results in a total count:

$$N_a(T) = \sum_i g_i n_i \quad (46)$$

where g_i is the random gain associated with the i th count. Thus, to make a decision based on $N_a(T)$, some knowledge of the random gain, g_i , should be known, specifically, the gain probability distribution given by Eq (44).

Repeating the logic used to determine the effect of output quantization developed in Chapter III, the count $N_a(T)$ can be thought of as the sum of J individual count terms, N_{ai} . Again, to characterize the channel, the transition probabilities for all of the possible channel output strings are required. The output from the channel will again be one of the 2^J possible J bit long strings, where J is the number of segments that T is partitioned into. Again, the unquantized system occurs when J equals one.

For each of the J segments of T , the MAP decision rule of Eq (26) will be used to determine whether the bit for that segment is a zero or a one. Substituting N_{ai} for N_i in Eq (26) gives:

Returning to the channel model, substituting Eqs (48) and (49) into Eq (47) gives:

$$\frac{\sum_{t=1}^{n-1} p(t|M_1)P_{t,n}}{\sum_{t=1}^{n-1} p(t|M_0)P_{t,n}} \begin{matrix} D_1 \\ > 1 \\ < \\ D_0 \end{matrix} \frac{\Pr\{M_0\}}{\Pr\{M_1\}} \quad (53)$$

The probability of t counts given M_1 with T portioned into J segments is given by Eq (27). Similarly, the probability of t counts given M_0 and J is given by Eq (28). Now, while Eq (53) is not easily solved directly, it can be solved by iteration, yielding a value, N_{0a} . This N_{0a} is analogous to N_0 developed in Chapter III for the ideal unity gain detector. Thus, if the count for any segment, n_i , is greater than N_{0a} , that segment's bit is set to one; if n_i is less than N_{0a} , the bit for the segment is set to zero; and again, Eq (18) is used if $n_i = N_{0a}$. As in Chapter III, this comparison is made for each of the J segment counts, n_i , until a J bit long string of zeros and ones is formulated. This string is the output of the channel model, and, once again, a "soft decision" is made.

To complete the characterization of the channel, the single bit crossover probability must be determined to enable the calculation of the final transition probabilities. These bit crossover probabilities for each segment are given by:

$$\begin{aligned}
\Pr\{D_1|M_0\} &= \Pr\{n_i > N_{0a}|M_0\} \\
&= \sum_{n=N_{0a}}^{\infty} \sum_{t=0}^{n-1} p(t|M_0)P_{t,n} = (1 - p_0)
\end{aligned} \tag{54}$$

and

$$\begin{aligned}
\Pr\{D_0|M_1\} &= \Pr\{n_i < N_{0a}|M_1\} \\
&= \sum_{t=0}^{N_{0a}-1} \sum_{n=t+1}^{N_{0a}} p(t|M_1)P_{t,n} = (1 - p_1)
\end{aligned} \tag{55}$$

The probabilities given by Eqs (54) and (55) are analogous to the probabilities given by Eqs (30) and (31) for the ideal unity gain detector system.

For an arbitrary J , the transition probability associated with a particular J bit long string is calculated by the procedure given in Chapter III:

- 1 - Let the number of ones in the J bit string equal v , then the number of zeros in the string is $J - v$;
- 2 - To determine the transition probability of the particular string, given M_1 was transmitted:

$$\Pr\{(J \text{ bit string})|M_1\} = p_1^v (1-p_1)^{J-v} \tag{32}$$

where $(1-p_1)$ is given by Eq (55);

- 3 - To determine the transition probability of the particular string, given M_0 was transmitted:

$$\Pr\{(J \text{ bit string})|M_0\} = p_0^{J-v}(1-p_0)^v \quad (33)$$

where $(1-p_0)$ is given by Eq (54).

A model which fully characterizes the channel employing an avalanche detector has now been developed. The next step is to determine the optimum post-detection processing required for the channel model.

Post-Detection Processing

The MAP decision rule of Eq (3) is once again the basis for developing the optimum post-detection processor. For any J bit string output by the channel the MAP decision rule gives:

$$\frac{\Pr\{X_1 X_2 \dots X_J | M_1\}}{\Pr\{X_1 X_2 \dots X_J | M_0\}} \underset{D_0}{\overset{D_1}{>}} \frac{\Pr\{M_0\}}{\Pr\{M_1\}} \quad (34)$$

where $X_1 X_2 \dots X_J$ is the J bit long string of zeros and ones.

Substituting Eqs (32) and (33) into Eq (34) gives:

$$\frac{p_1^v (1-p_1)^{J-v}}{p_0^{J-v} (1-p_0)^v} \underset{D_0}{\overset{D_1}{>}} \frac{\Pr\{M_0\}}{\Pr\{M_1\}} \quad (35)$$

where v is the number of ones in the J bit string. This is identical to the results developed in Chapter III for the ideal unity gain detector. Similarly, L_0 as defined by:

$$v \begin{matrix} D_1 \\ > \\ < \\ D_0 \end{matrix} \frac{\ln \left(\frac{\Pr\{M_0\}}{\Pr\{M_1\}} \right) - J \ln \left(\frac{(1 - p_0)}{p_0} \right)}{\ln \left(\frac{p_0 p_1}{(1 - p_0)(1 - p_1)} \right)} = L_0 \quad (36)$$

will be used as the decision maker of Figure 6. Thus, the major difference between the avalanche detector system and the ideal unity gain detector system is in the calculation of the transition probability for each of the J individual bits, as is evident by comparing Eq (54) with Eq (30) and Eq (55) with Eq (31).

Probability of Error

The system probability of error is given by:

$$P(E) = \Pr\{D_0|M_1\}\Pr\{M_1\} + \Pr\{D_1|M_0\}\Pr\{M_0\} \quad (5)$$

which reduces to:

$$P(E) = \left[\sum_{v=0}^{\lfloor L_0 \rfloor} \binom{J}{v} p_1^v (1 - p_1)^{J - v} \right] \Pr\{M_1\} + \left[\sum_{v=\lceil L_0 \rceil}^J \binom{J}{v} p_0^{J - v} (1 - p_0)^v \right] \Pr\{M_0\} \quad (37)$$

as was the case for the ideal unity gain detector.

Summary

The addition of an avalanche detector into the system adds a random factor into the computations and thus adds

complexity to the channel model. By using the probability distribution for $P_{n,n+r}$ developed by McIntyre, the channel can be characterized, and probability of error data is readily calculated. [It should be noted that a discrepancy was noted in the paper by McIntyre (Ref 12). Using Eq (44) to calculate $P_{n,n+r}$, the results obtained did not agree with Figure 3 of McIntyre's work. If, however, the results of Eq (44) were multiplied by n , Figure 3 was reproduced. For the purposes of this report, the results of Eq (44) were used in the calculations where $P_{n,n+r}$ were required.]

Figure 9 shows a simple flowchart used in calculating the system probability of error. Appendix A, Figure 19 is a listing of the BASIC language computer program used to compute data. Appendix B, Table IV lists calculated data for the avalanche detector system.

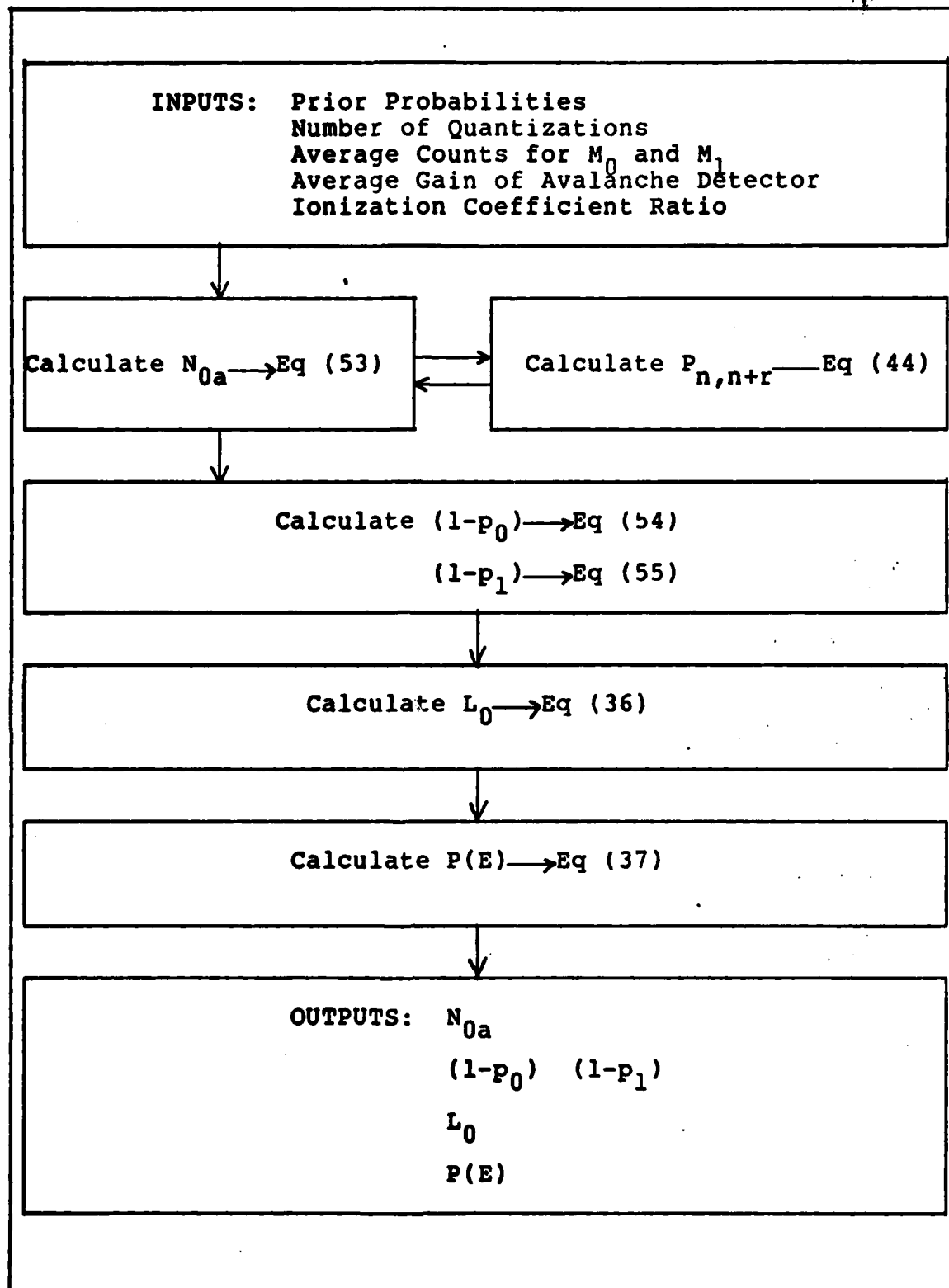


Figure 9. Avalanche Detector, Probability of Error Flowchart

VI Conclusions

General Information

Several equations have been developed to assist in analyzing the Multilevel Amplitude Keyed direct detection optical communication system. The discrete nature of the integrate-and-dump receiver and the counting process and how the equations are affected by the discreteness lead to some important conclusions.

To characterize the ideal unity gain detector channel, the threshold $N_{0,J}$ was defined to be:

$$N_{0,J} = \frac{\frac{\mu_1 - \mu_0}{J} + \ln \left(\frac{\Pr\{M_0\}}{\Pr\{M_1\}} \right)}{\ln \left(\frac{\mu_1}{\mu_0} \right)} \quad (29)$$

This threshold determined whether the bit for a segment was to be a zero or a one. It is important to note that for $N_{0,J} < 0$, the bit will always be set to one; M_1 will always be decided; and the system probability of error will be the prior probability of M_0 . This will occur for $M_0 < M_1$, $\mu_0 < \mu_1$, and large J . For $M_0 > M_1$ and $\mu_0 < \mu_1$, this situation is reversed; $N_{0,J}$ is positive and more bits will be set to zero. Eventually, for $M_0 \gg M_1$, and small J , all the bits will be set to zero; M_0 will always be decided; and the system probability of error will equal the prior probability of M_1 . The second important fact concerning $N_{0,J}$ is

that a threshold of 2.99 will give equivalent results as a threshold of 2.01. Clearly, due to the discrete nature of the counting process, some information about the relative position between a threshold and the count is lost.

A similar situation exists for L_0 , the threshold for both ideal unity gain and avalanche detector systems, given by:

$$L_0 = \frac{\ln \left(\frac{\Pr\{M_0\}}{\Pr\{M_1\}} \right) - J \ln \left(\frac{1 - p_0}{p_0} \right)}{\ln \left(\frac{p_0 p_1}{(1 - p_0)(1 - p_1)} \right)} \quad (36)$$

If $L_0 \leq 0$, M_1 is always decided, and the probability of error equals the prior probability of M_0 . If $L_0 > J$, M_0 is always decided, and the probability of error equals the prior probability of M_1 . Likewise, a threshold of 2.99 will result in the same decision as a threshold of 2.01. Thus, $N_{0,J}$ and L_0 are both affected in a similar manner by the discrete nature of the counting process.

The final equation of interest is:

$$\frac{\sum_{t=1}^{n-1} p(t|M_1)P_{t,n}}{\sum_{t=1}^{n-1} p(t|M_0)P_{t,n}} \begin{matrix} D_1 \\ > 1 \\ < \\ D_0 \end{matrix} \begin{matrix} \Pr\{M_0\} \\ \Pr\{M_1\} \end{matrix} \quad (53)$$

This equation can be solved by iteration for n , given a value N_{0a} . The N_{0a} is a threshold, comparable to $N_{0,J}$, but is used in analysis of an avalanche detector system. This

equation may not yield a threshold for certain values of prior probabilities and average counts associated with M_0 and M_1 . For example, given equilikely priors, Eq (53) reduces to:

$$\frac{\sum_{t=1}^{n-1} p(t|M_1)P_{t,n}}{\sum_{t=1}^{n-1} p(t|M_0)P_{t,n}} \begin{matrix} D_1 \\ > 1 \\ < \\ D_0 \end{matrix} \quad (54)$$

Since $P_{t,n}$ will be the same value in both the numerator and the denominator for any value of t and n , in order to solve Eq (54) for N_{0a} , $p(t|M_0)$ must be greater than $p(t|M_1)$ for some integer value of t . Using Eqs (8) and (9), it can be shown that this is not necessarily the case. [For example: if $\mu_0 = .2$ and $\mu_1 = 1$, then $p(t|M_0) < p(t|M_1)$ for all integer values of t .] Thus, care must be used in selecting values for μ_0 and μ_1 when analyzing the avalanche detector system.

Ideal Detector, Quantized Output

Using the calculated data from Table II, Appendix B, two distinct conclusions concerning probability of error can be made. First, as shown in Figure 10, given μ_0 , the average count for M_0 , as μ_1 gets further from μ_0 , the probability of error decreases. This is as expected because as the "distance" between two signals increases, the probability of making an error should decrease. The second

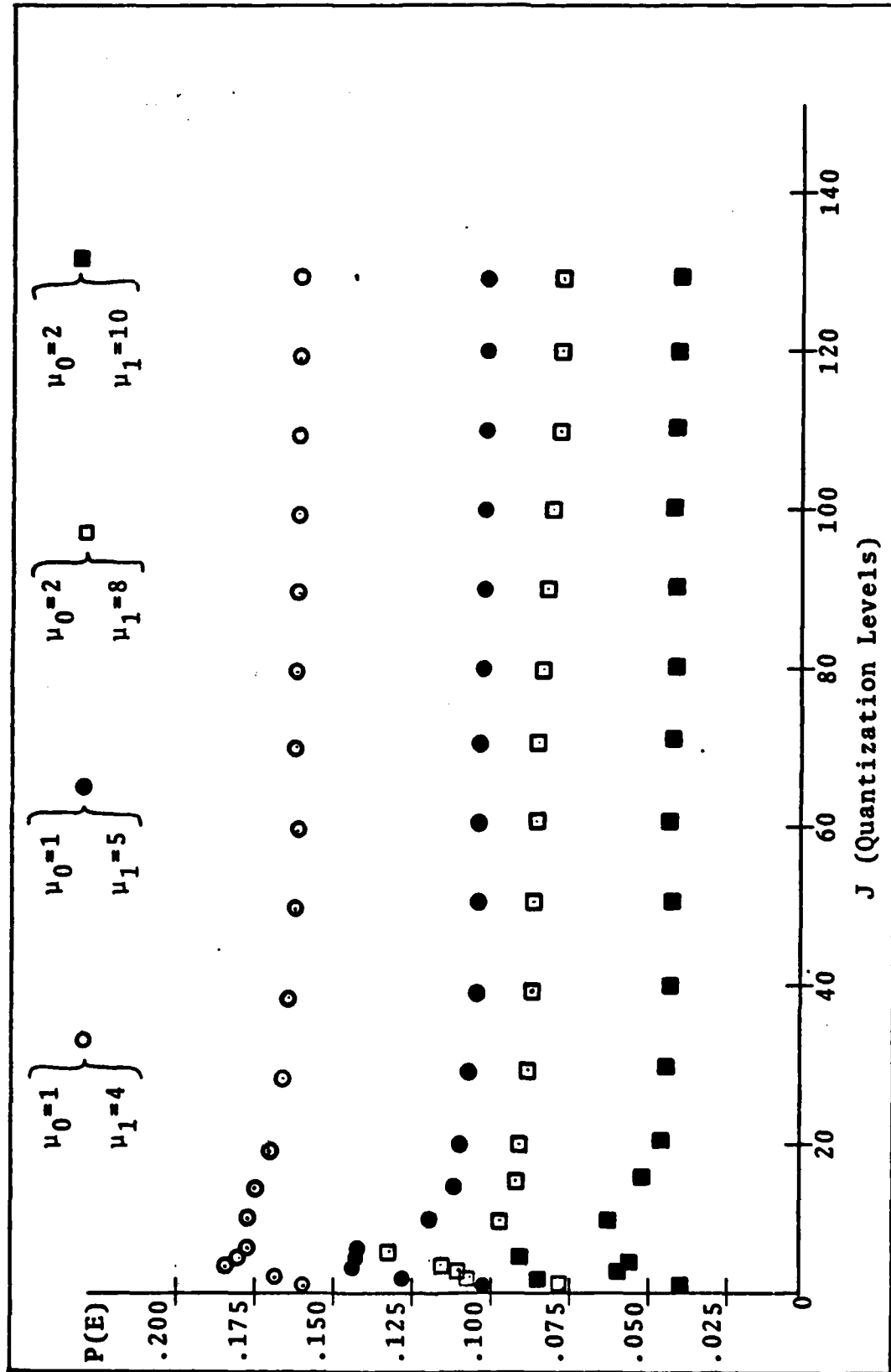


Figure 10. Probability of Error vs Quantizations for Ideal Detector
 (μ_0 constant : μ_1 varying)

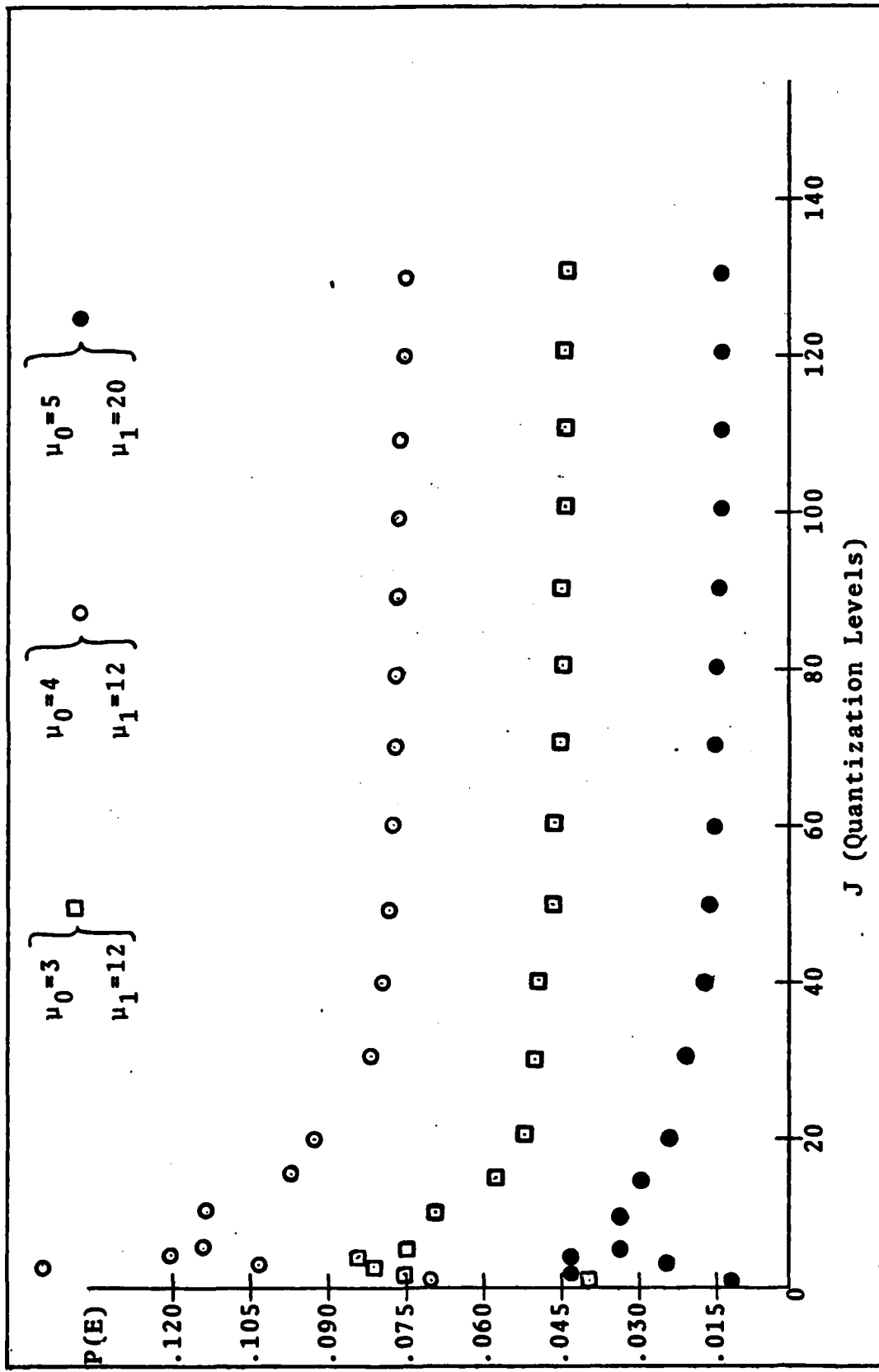


Figure 11. Probability of Error vs Quantizations for Ideal Detector (μ_0, μ_1 varying)

conclusion is not as obvious. As shown in Figure 11, as the quantizations increase, the probability of error first increases and then decreases asymptotically to the level for unquantized output. The reason for this is that by quantizing the output, a "hard decision" channel became a "soft decision" channel where probability of error is no longer a valid decision criterion.

Cutoff Rate Analysis

The conclusion made by examining the cutoff rates has already been stated by examining Eq (41). As shown in Figure 12, for the ideal unity gain detector, and Figure 13, for the avalanche detector, as the symmetric cutoff rate \tilde{R}_0 increases, the probability of error decreases. Thus, while probability of error has no meaning for "soft decision" channels, examination of the cutoff rate, specifically maximizing the cutoff rate, will result in a criterion that can effectively be used to minimize probability of error.

Avalanche Detector, Quantized Output

Plotting the data from Table IV, Appendix B, in Figure 14 shows that the minimum probability of error is not obtained with unquantized output, as it was for the ideal unity gain detector. The value of J that returns minimum probability of error increases as the distance between μ_0 and μ_1 increases. Additionally, the value of J that produces minimum probability of error also results in N_{0a} being

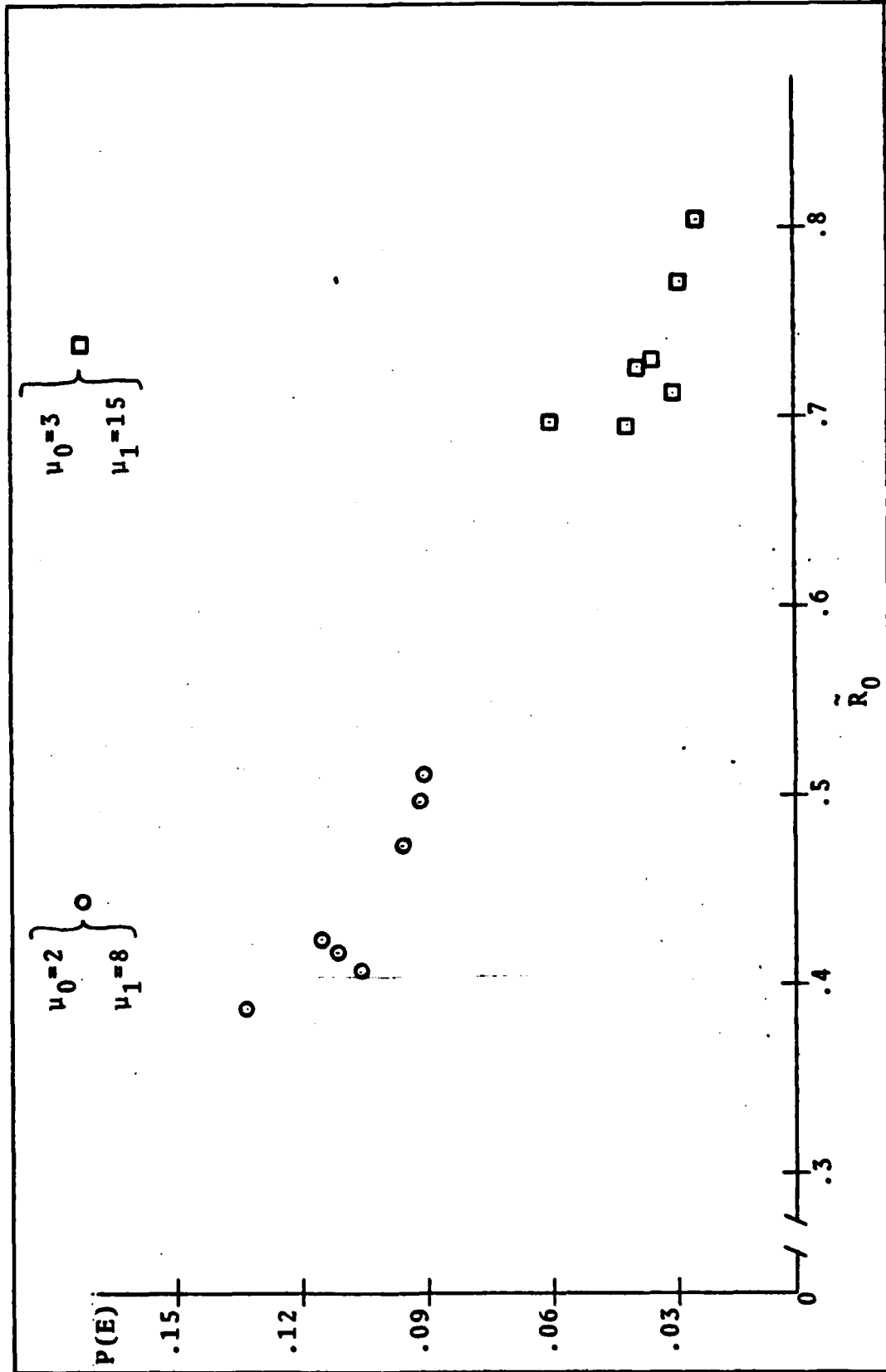


Figure 12. Probability of Error vs Symmetric Cutoff Rate for Ideal Detector

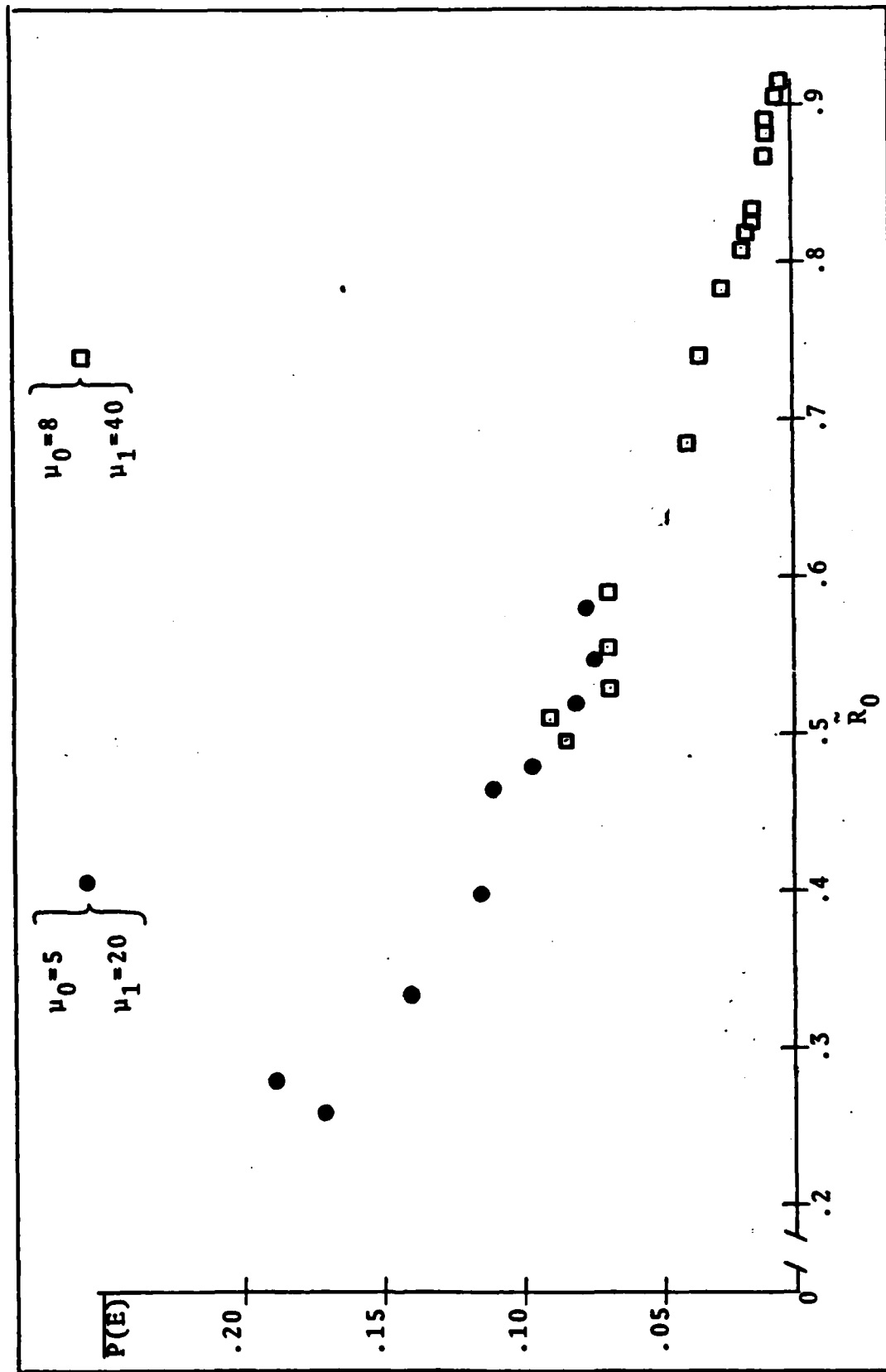


Figure 13. Probability of Error vs Symmetric Cutoff Rate for Avalanche Detector

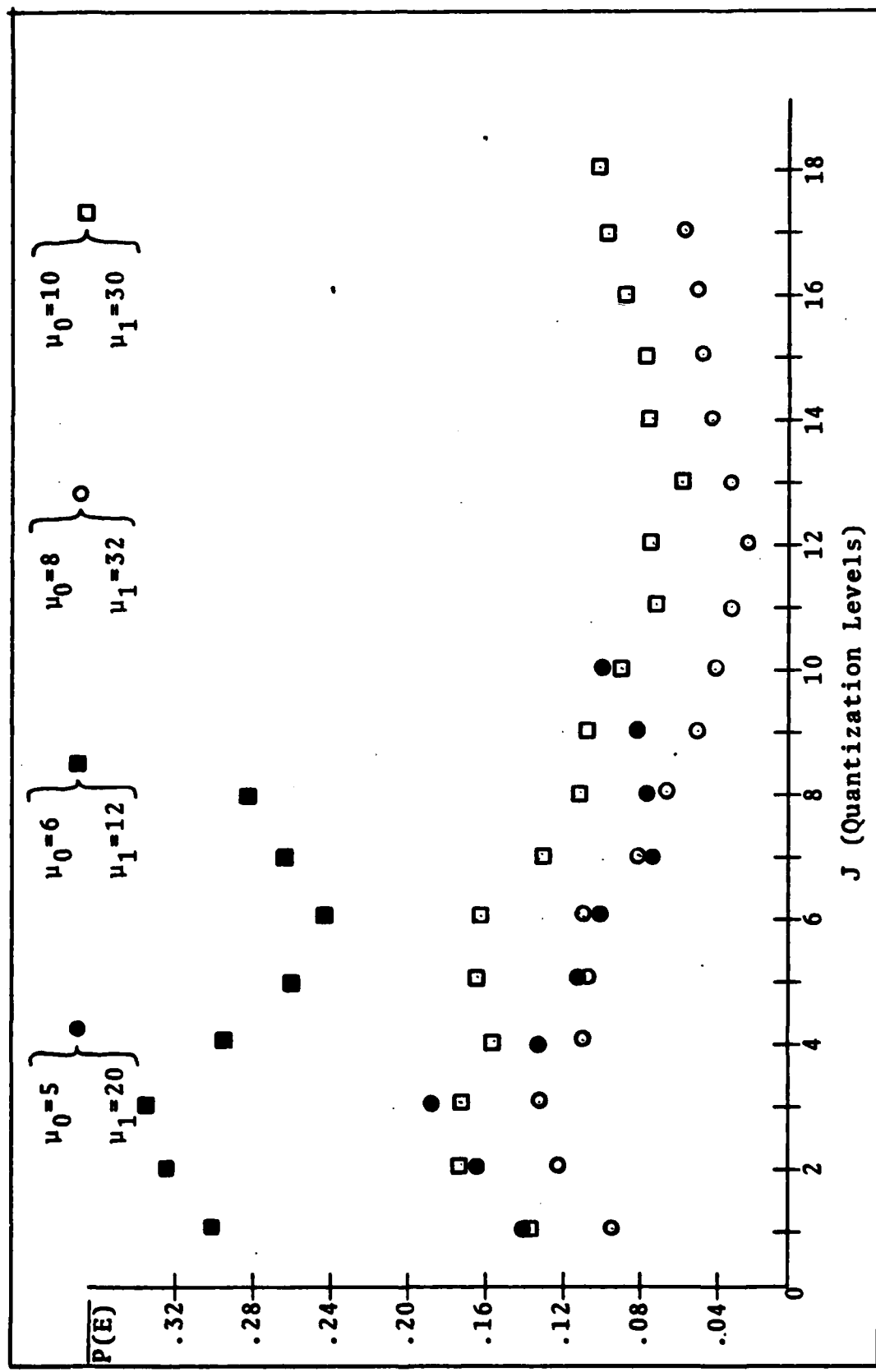


Figure 14. Probability of Error vs Quantizations for Avalanche Detectors

a minimum value and L_0 being a maximum value. The data from Table IV is in agreement with the ideal unity gain detector data in that as the distance between μ_0 and μ_1 increases, the probability of error decreases, as expected.

Topics for Future Research

An obvious extension of this paper would be to abandon the MAP decision rule and try to improve the probability of error results by using a cutoff rate criterion when the output is quantized and a "soft decision" channel exists. The cutoff rate criterion results could be compared to the results obtained by the MAP criterion of this paper to demonstrate the benefits of using cutoff rate criterion for "soft decisions."

Another area of interest would be expanding the study of the avalanche detector system and attempting to determine what level of quantization would return a minimum probability of error for any given M_0 and M_1 characteristics.

These are just two areas barely touched in this work that may provide additional depth of knowledge into the field of optical communications.

Bibliography

1. Bar-David, Israel. "Communication under the Poisson Regime," IEEE Transactions on Information Theory, IT-15 (1): 31-37 (January 1969).
2. Carpinella, Lt Col Ronald J., Professor of Electrical Engineering. Lecture materials distributed in EE 6.72, Signal Processing for Electro-Optic Systems. School of Engineering, Air Force Institute of Technology, Wright-Patterson AFB, Ohio, 1982.
3. Chan, Vincent W. S. "Coding for the Turbulent Atmospheric Optical Channel," IEEE Transactions on Communications, COM-30 (1): 269-275 (January 1982).
4. Conradi, Jan. "The Distribution of Gains in Uniformly Multiplying Avalanche Photodiodes: Experimental," IEEE Transactions on Electron Devices, ED-19 (6): 713-718 (June 1972).
5. DiFranco, J. V. and W. L. Rubin. Radar Detection. Englewood Cliffs: Prentice-Hall, 1968.
6. Gagliardi, Robert M. and Sherman Karp. Optical Communications. New York: John Wiley and Sons, 1976.
7. Gallager, Robert G. Information Theory and Reliable Communication. New York: John Wiley and Sons, 1968.
8. Hoversten, E. V. "Optical Communication Theory," in Laser Handbook, F. T. Arecchi and E. O. Schulz-DuBois, Eds. Amsterdam: North Holland, 1972.
9. Karp, S. and J. R. Clark. "Photon Counting: A Problem in Classical Noise Theory," IEEE Transactions on Information Theory, IT-16 (6): 672-680 (November 1970).
10. Lee, Lin-Nan. "On Optimal Soft-Decision Demodulation," IEEE Transactions on Information Theory, IT-22 (4): 437-444 (July 1976).
11. Massey, James L. "Coding and Modulation in Digital Communications," Proceedings of the International Zurich Seminar on Digital Communications. E2(1)-E2(4), 1974.
12. McIntyre, Robert J. "The Distribution of Gains in Uniformly Multiplying Avalanche Photodiodes: Theory," IEEE Transactions on Electron Devices, ED-19 (6): 703-713 (June 1972).

13. Melsa, James L. and David L. Cohn. Decision and Estimation Theory. New York: McGraw-Hill, 1978.
14. Personick, S. D. "New Results on Avalanche Multiplication Statistics with Applications to Optical Detection," Bell System Technical Journal, 50 (10): 167-189 (January 1971).
15. ----- . "Photodetectors for Fiber Systems," in Fundamentals of Optical Fiber Communications, Michael K. Barnoski, Ed. New York: Academic Press, 1976.
16. ----- . "Statistics of a General Class of Avalanche Detectors With Applications to Optical Communication," Bell System Technical Journal, 50 (10): 3075-3095 (December 1971).
17. Snyder, Donald L. and Ian B. Rhodes. "Some Implications of the Cutoff-Rate Criterion for Coded Direct-Detection Optical Communication Systems," IEEE Transactions on Information Theory, IT-26 (3): 327-338 (May 1980).
18. Snyder, Donald L. Random Point Processes. New York: John Wiley and Sons, 1975.
19. Van Trees, Harry L. Detection, Estimation, and Modulation Theory, Part I. New York: John Wiley and Sons, 1968.
20. ----- . Detection, Estimation, and Modulation Theory, Part III. New York: John Wiley and Sons, 1971.
21. Viterbi, A. J. and J. K. Omura. Principles of Digital Communication and Coding. New York: McGraw-Hill, 1979.
22. Viterbi, Andrew J. "Error Bounds for Convolutional Codes and an Asymptotically Optimum Decoding Algorithm," IEEE Transactions on Information Theory, IT-13 (2): 260-269 (April 1967).
23. Webb, P. P., R. J. McIntyre and J. Conradi. "Properties of Avalanche Photodiodes," RCA Review, 35 (2): 234-278 (June 1974).
24. Wozencraft, John M. and Irwin Mark Jacobs. Principles of Communication Engineering. New York: John Wiley and Sons, 1965.
25. Wozencraft, J. M. and R. S. Kennedy. "Modulation and Demodulation for Probabilistic Coding," IEEE Transactions on Information Theory, IT-12 (3): 291-297 (July 1966).

Appendix A
Computer Programs

Ideal Detector, Quantized Output

Figure 15 is the listing of the BASIC computer program used to calculate the data listed in Table II of Appendix B. A sample of the output from this program is given in Figure 16. The program requires the prior probabilities of messages M_0 and M_1 , the number of segments in the interval T and the average count for messages M_0 and M_1 as input variables. As output, the program returns N_0 [calculated by Eq (29)], the bit transition probabilities, [calculated by Eqs (30) and (31)], L_0 [calculated by Eq (36)], and the system probability of error [calculated by Eq (37)].

```

1Ø LPRINT "THEESIS1 - THIS PROGRAM CALCULATES:"
2Ø LPRINT "      NØ - THE NUMBER OF COUNTS PER SEGMENT USED
           TO DETERMINE A 1 OR Ø FOR THAT
           SEGMENT"
3Ø LPRINT "      IF N > NØ   DECIDE 1 FOR THAT SEGMENT"
4Ø LPRINT "      IF N < NØ   DECIDE Ø FOR THAT SEGMENT"
5Ø LPRINT "      CP1 - THE PROBABILITY OF DECIDING A 1 FOR A
           SEGMENT GIVEN MESSAGE 1 WAS SENT"
6Ø LPRINT "      CPØ - THE PROBABILITY OF DECIDING A 1 FOR A
           SEGMENT GIVEN MESSAGE Ø WAS SENT"
7Ø LPRINT "      LØ - THE NUMBER OF SEGMENTS WHERE A 1 WAS
           DECIDED REQUIRED TO MAKE THE FINAL
           DECISION THAT MESSAGE 1 WAS SENT"
8Ø LPRINT "      IF MORE THAN LØ OF THE J SEGMENTS ARE
           1 THEN DECIDE MESSAGE 1 WAS SENT"
9Ø LPRINT "      IF LESS THAN LØ OF THE J SEGMENTS ARE
           1 THEN DECIDE MESSAGE Ø WAS SENT"
1ØØ LPRINT "      P OF E - THE OVERALL SYSTEM PROBABILITY OF
           ERROR"
11Ø LPRINT "GIVEN THE INPUTS:"
12Ø LPRINT "      PRØ - THE PRIOR PROBABILITY OF MESSAGE Ø"
13Ø LPRINT "      J - THE NUMBER OF SEGMENTS T IS DIVIDED
           INTO"
14Ø LPRINT "      MØ - THE AVERAGE COUNT FOR MESSAGE Ø BEING
           SENT"
15Ø LPRINT "      M1 - THE AVERAGE COUNT FOR MESSAGE 1 BEING
           SENT"
16Ø LPRINT
17Ø LPRINT
18Ø LPRINT
19Ø LPRINT "      J  PRØ  PR1  MØ  M1",,"  NØ", "  CPØ", "
           CP1", "  LØ", "  P OF E"
2ØØ INPUT "ENTER PRIOR PROBABILITY OF MESSAGE Ø"; PRØ
21Ø INPUT "ENTER NUMBER OF SEGMENTS IN T"; J
22Ø INPUT "ENTER AVERAGE COUNT FOR MESSAGE Ø"; MØ
23Ø INPUT "ENTER AVERAGE COUNT FOR MESSAGE 1"; M1
24Ø PR1 = 1 - PRØ
25Ø REM
26Ø REM   CALCULATE NØ
27Ø REM
28Ø NØ = ((LOG (PRØ/PR1)) + (M1-MØ)/J) / LOG(M1/MØ)
29Ø IF NØ<=Ø GOTO 78Ø
3ØØ REM
31Ø REM   CALCULATE CPØ AND CP1
32Ø REM
33Ø SMØ = Ø
34Ø SM1 = Ø
35Ø FOR N = Ø TO INT(NØ)

```

Figure 15. Ideal Detector, Quantized Output Program Listing
(Sheet 1 of 2)

```

36Ø TERMØ = (MØ/J)^N
37Ø TERM1 = (M1/J)^N
38Ø FOR A = 1 TO N
39Ø TERMØ = TERMØ/A
40Ø TERM1 = TERM1/A
41Ø NEXT A
42Ø SMØ = SMØ + TERMØ
43Ø SM1 = SM1 + TERM1
44Ø NEXT
45Ø CPØ = 1 - (SMØ*(EXP(-MØ/J)))
46Ø CP1 = SM1*(EXP(-M1/J))
47Ø REM
48Ø REM CALCULATE LØ
49Ø REM
50Ø LØ = ((LOG(PRØ/PR1))- J*(LOG(CP1/(1-CPØ))))/
LOG(((1-CPØ)*(1-CP1))/(CPØ*CP1))

51Ø REM
52Ø REM CALCULATE P OF E
53Ø REM
54Ø SUM1 = Ø
55Ø FOR R = Ø TO INT(LØ)
56Ø GOSUB 67Ø
57Ø SUM1 = SUM1 + (NUMBER)*(CP1^(J-R))*(1-CP1)^R
58Ø NEXT
59Ø SUMØ = Ø
60Ø FOR R = INT(LØ+1) TO J
61Ø GOSUB 67Ø
62Ø SUMØ = SUMØ + (NUMBER)*((1-CPØ)^(J-R))*CPØ^R
63Ø NEXT
64Ø ERRPROB = SUM1*PR1 + SUMØ*PRØ
65Ø LPRINT J;" ";PRØ;" ";PR1;" ";MØ;" ";M1,,NØ,CPØ,CP1,
LØ, ERRPROB

66Ø END
67Ø NUMBER = 1
68Ø IF J = R GOTO 77Ø
69Ø B = J
70Ø C = J - R
71Ø NUMBER = NUMBER*B/C
72Ø B = B - 1
73Ø C = C - 1
74Ø IF B = R THEN B = 1
75Ø IF C = Ø THEN C = 1
76Ø IF B > C GOTO 71Ø
77Ø RETURN
78Ø IF PRØ<PR1 THEN CPØ=1:CP1=Ø:LØ=Ø:ERRPROB=PRØ ELSE
CPØ=Ø:CP1=1:LØ=J:ERRPROB=PR1
79Ø GOTO 65Ø

```

Figure 15. Ideal Detector, Quantized Output Program Listing
(Sheet 2 of 2)

THESIS1 - THIS PROGRAM CALCULATES:
 NØ - THE NUMBER OF COUNTS PER SEGMENT USED TO DETERMINE
 A 1 OR Ø FOR THAT SEGMENT
 IF N > NØ DECIDE 1 FOR THAT SEGMENT
 IF N < NØ DECIDE Ø FOR THAT SEGMENT
 CP1 - THE PROBABILITY OF DECIDING A Ø FOR A SEGMENT
 GIVEN MESSAGE 1 WAS SENT
 CPØ - THE PROBABILITY OF DECIDING A 1 FOR A SEGMENT
 GIVEN MESSAGE Ø WAS SENT
 LØ - THE NUMBER OF SEGMENTS WHERE A 1 WAS DECIDED
 REQUIRED TO MAKE THE FINAL DECISION THAT MESSAGE 1
 WAS SENT
 IF MORE THAN LØ OF THE J SEGMENTS ARE 1 THEN
 DECIDE MESSAGE 1 WAS SENT
 IF LESS THAN LØ OF THE J SEGMENTS ARE 1 THEN
 DECIDE MESSAGE Ø WAS SENT
 P OF E - THE OVERALL SYSTEM PROBABILITY OF ERROR
 GIVEN THE INPUTS:
 PRØ - THE PRIOR PROBABILITY OF MESSAGE Ø
 J - THE NUMBER OF SEGMENTS T IS DIVIDED INTO
 MØ - THE AVERAGE COUNT FOR MESSAGE Ø BEING SENT
 M1 - THE AVERAGE COUNT FOR MESSAGE 1 BEING SENT

<u>J</u>	<u>PRØ</u>	<u>PR1</u>	<u>MØ</u>	<u>M1</u>	<u>NØ</u>
1Ø	.5	.5	5	25	1.24267
	<u>CPØ</u>	<u>CP1</u>	<u>LØ</u>	<u>P OF E</u>	
	.Ø9Ø2Ø4	.287297	3.58Ø16	8.54147E-Ø3	

Figure 16. Ideal Detector, Quantized Output Program
Sample Output

Cutoff Rate Calculations

Figure 17 is the listing of the BASIC computer program used to calculate the data listed in Table III of Appendix B. A sample of the output from this program is given in Figure 18. The program requires the bit transition probabilities [calculated by Eqs (27) and (28)] and the number of segments in the interval T as input variables. The program returns the symmetric cutoff rate [calculated by Eq (40)] and the system probability of error bound [calculated by Eq (43)] as output.

```

1Ø LPRINT "THEESIS2 - THIS PROGRAM CALCULATES:"
2Ø LPRINT "      RØ - THE SYMMETRIC CUT-OFF RATE"
4Ø LPRINT "GIVEN THE INPUTS:"
5Ø LPRINT "      CP1 - THE PROBABILITY OF DECIDING A Ø FOR A
      SEGMENT GIVEN MESSAGE 1 WAS SENT"
6Ø LPRINT "      CPØ - THE PROBABILITY OF DECIDING A 1 FOR A
      SEGMENT GIVEN MESSAGE Ø WAS SENT"
7Ø LPRINT "      J - THE NUMBER OF SEGMENTS T IS DIVIDED
      INTO"

8Ø LPRINT
9Ø LPRINT
1ØØ LPRINT
11Ø LPRINT " J      CPØ      CP1", " RØ"
12Ø INPUT "ENTER NUMBER OF SEGMENTS IN T"; J
13Ø INPUT "ENTER CROSSOVER PROBABILITY FOR HØ"; CPØ
14Ø INPUT "ENTER CROSSOVER PROBABILITY FOR H1"; CP1
15Ø RSUM = Ø
16Ø REM
17Ø REM      CALCULATE RØ
18Ø REM
19Ø FOR L = Ø TO J
2ØØ GOSUB 31Ø
21Ø MSUM = NUMBER * (SQR((1-CPØ)^(J-L) *(CPØ^L)) +
      SQR((CP1^(J-L))*(1-CP1)^L))^2
22Ø RSUM = RSUM + MSUM
23Ø NEXT
24Ø RØ = 1 - ((LOG(RSUM/2))/LOG (2))
29Ø LPRINT J;" ";CPØ;" ";CP1;" ";RØ
3ØØ END
31Ø NUMBER = 1
32Ø IF J = L GOTO 41Ø
33Ø B = J
34Ø C = J - L
35Ø NUMBER = NUMBER*B/C
36Ø B = B - 1
37Ø C = C - 1
38Ø IF B = L THEN B = 1
39Ø IF C = Ø THEN C = 1
4ØØ IF B > C GOTO 35Ø
41Ø RETURN

```

Figure 17. Cutoff Rate Calculations Program Listing

THESIS2 - THIS PROGRAM CALCULATES:
 R_{β} - THE SYMMETRIC CUT-OFF RATE
 GIVEN THE INPUTS:
 CP_1 - THE PROBABILITY OF DECIDING A β FOR A SEGMENT
 GIVEN MESSAGE 1 WAS SENT
 CP_{β} - THE PROBABILITY OF DECIDING A 1 FOR A SEGMENT
 GIVEN MESSAGE β WAS SENT
 J - THE NUMBER OF SEGMENTS T IS DIVIDED INTO

<u>J</u>	<u>CPβ</u>	<u>CP₁</u>	<u>Rβ</u>
5	.32968	.135335	.5 β 8227

Figure 18. Cutoff Rate Calculations Program Sample Output

Avalanche Detector, Quantized Output

Figure 19 is the listing of the BASIC computer program used to calculate the data listed in Table IV of Appendix B. A sample of the output from this program is given in Figure 20. The program requires the prior probabilities of messages M_0 and M_1 , the number of segments in the interval T , the average count for messages M_0 and M_1 , the average gain of the avalanche detector and the ionization coefficient ratio of the avalanche detector as input variables. The output consists of N_{0a} [calculated from Eq (53)], the bit transition probabilities [calculated from Eqs (54) and (55)], L_0 [calculated by Eq (36)], and the system probability of error [calculated by Eq (37)].

```

1Ø LPRINT "THESIS3 - THIS PROGRAM CALCULATES;"
2Ø LPRINT "      MO - THE NUMBER OF COUNTS PER SEGMENT USED
          TO DETERMINE A 1 OR Ø FOR THAT
          SEGMENT"
3Ø LPRINT "      IF N > MO  DECIDE 1 FOR THAT SEGMENT"
4Ø LPRINT "      IF N < MO  DECIDE Ø FOR THAT SEGMENT"
5Ø LPRINT "      CP1 - THE PROBABILITY OF DECIDING A Ø FOR A
          SEGMENT GIVEN MESSAGE 1 WAS SENT"
6Ø LPRINT "      CPØ - THE PROBABILITY OF DECIDING A 1 FOR A
          SEGMENT GIVEN MESSAGE Ø WAS SENT"
7Ø LPRINT "      LØ - THE NUMBER OF SEGMENTS WHERE A 1 WAS
          DECIDED REQUIRED TO MAKE THE FINAL
          DECISION THAT MESSAGE 1 WAS SENT"
8Ø LPRINT "      IF MORE THAN LØ OF THE J SEGMENTS ARE
          1 THEN DECIDE MESSAGE 1 WAS SENT"
9Ø LPRINT "      IF LESS THAN LØ OF THE J SEGMENTS ARE
          1 THEN DECIDE MESSAGE Ø WAS SENT"
1ØØ LPRINT " P OF E - THE OVERALL SYSTEM PROBABILITY OF
          ERROR"
11Ø LPRINT "GIVEN THE INPUTS:"
12Ø LPRINT "      PRØ - THE PRIOR PROBABILITY OF MESSAGE Ø"
13Ø LPRINT "      J - THE NUMBER OF SEGMENTS T IS DIVIDED
          INTO"
14Ø LPRINT "      MØ - THE AVERAGE COUNT FOR MESSAGE Ø BEING
          SENT"
15Ø LPRINT "      M1 - THE AVERAGE COUNT FOR MESSAGE 1 BEING
          SENT"
16Ø LPRINT "      M - THE AVERAGE GAIN OF THE AVALANCHE
          DETECTOR"
17Ø LPRINT "      K - THE HOLE IONIZATION COEFFICIENT TO
          ELECTRON IONIZATION COEFFICIENT RATIO"
18Ø LPRINT
19Ø LPRINT
2ØØ LPRINT
21Ø INPUT "ENTER PRIOR PROBABILITY OF MESSAGE Ø"; PRØ
22Ø INPUT "ENTER NUMBER OF SEGMENTS IN T"; J
23Ø INPUT "ENTER AVERAGE COUNT FOR MESSAGE HØ"; MØ
24Ø INPUT "ENTER AVERAGE COUNT FOR MESSAGE H1"; M1
25Ø INPUT "ENTER AVERAGE GAIN FOR THE AVALANCHE DETECTOR"; M
26Ø INPUT "ENTER HOLE IONIZATION COEFFICIENT TO ELECTRON
          IONIZATION COEFFICIENT RATIO"; K
27Ø GOSUB 48Ø
28Ø REM
29Ø REM   CALCULATE CPØ AND CP1
3ØØ REM
31Ø SUMØ = Ø
32Ø CP1 = Ø

```

Figure 19. Avalanche Detector, Quantized Output
Program Listing
(Sheet 1 of 3)

```

33Ø FOR NI = 1 TO INT(MO)-1
34Ø FOR MCT = NI+1 TO INT(MO)
35Ø GOSUB 81Ø
36Ø TERMØ = PØ(NI) * PNMO
37Ø TERM1 = P1(NI) * PNMO
38Ø SUMØ = SUMØ + TERMØ
39Ø CP1 = CP1 + TERM1
40Ø NEXT MCT
41Ø NEXT NI
42Ø CP1 = CP1 + P1(Ø)
43Ø CPØ = 1 - (SUMØ + PØ(Ø))
44Ø GOTO 85Ø
45Ø REM
46Ø REM      CALCULATE MO
47Ø REM
48Ø PR1 = 1 - PRØ
49Ø DIM PØ(INT(M1*M/J)), P1(INT(M1*M/J))
50Ø PØ(Ø) = EXP(-MØ/J)
51Ø P1(Ø) = EXP(-M1/J)
52Ø FOR N = 1 TO (INT(M1*M/J)-1)
53Ø PØ(N) = PØ(N-1)*(MØ/(J*N))
54Ø P1(N) = P1(N-1)*(M1/(J*N))
55Ø NEXT N
56Ø RIGHT = PRØ/PR1
57Ø MO = M
58Ø DIFFLT = 1E+37
59Ø SUM = Ø
60Ø TOPSUM = Ø
61Ø BOTSUM = Ø
62Ø FOR NI = 1 TO INT(MO-.ØØ1)
63Ø MCT = MO
64Ø GOSUB 81Ø
65Ø TOP = P1(NI)*PNMO
66Ø BOT = PØ(NI)*PNMO
67Ø TOPSUM = TOPSUM + TOP
68Ø BOTSUM = BOTSUM + BOT
69Ø NEXT NI
70Ø LEFT = TOPSUM/BOTSUM
71Ø DIFF = RIGHT - LEFT
72Ø IF ABS(DIFF) > ABS(DIFFLT) GOTO 76Ø ELSE DIFFLT = DIFF
73Ø LMO = MO
74Ø IF DIFF > Ø THEN MO = 1.1*MO ELSE MO = .9*MO
75Ø GOTO 59Ø
76Ø MO = (DIFFLT/(DIFFLT-DIFF))*(MO-LMO)+LMO
77Ø RETURN
78Ø REM
79Ø REM      CALCULATE PNMO

```

Figure 19. Avalanche Detector, Quantized Output
Program Listing
(Sheet 2 of 3)

```

800 REM
810 F = MCT/(NI*M)
820 R = MCT - NI
830 PNMO = (NI/((6.28*MCT*(NI+K*R)*R)^.5))*((1-(NI*(F-1/R))
      ^R)*((1+(NI*(1-K)*(F-1)/(NI+K*R)))^((NI+K*R)/
      (1-K)))
840 RETURN
850 REM
860 REM      CALCULATE LØ
870 REM
880 LØ = ((LOG(PRØ/PR1))- J*(LOG(CP1/(1-CPØ))))/
      LOG(((1-CPØ)*(1-CP1))/(CPØ*CP1))
890 REM
900 REM      CALCULATE P OF E
910 REM
920 SUM1 = Ø
930 FOR R = Ø TO INT(LØ)
940 GOSUB 1060
950 SUM1 = SUM1 + (NUMBER)*(CP1^(J-R))*(1-CP1)^R
960 NEXT
970 SUMØ = Ø
980 FOR R = INT(LØ+1) TO J
990 GOSUB 1060
1000 SUMØ = SUMØ + (NUMBER)*((1-CPØ)^(J-R))*CPØ^R
1010 NEXT
1020 ERRPROB = SUM1*PR1 + SUMØ*PRØ
1030 LPRINT " J      PRØ      PR1      MØ      M1      K      M", "      MO",
      "      CPØ", "      CP1", "      LØ", "      P OF E"
1040 LPRINT J; "      ";PRØ; "      ";PR1; "      ";MØ; "      ";M1; "      ";K; "
      ";M; "      ",MO,CPØ,CP1,LØ,ERRPROB
1050 END
1060 NUMBER = 1
1070 IF J = R GOTO 1160
1080 B = J
1090 C = J - R
1100 NUMBER = NUMBER*B/C
1110 B = B - 1
1120 C = C - 1
1130 IF B = R THEN B = 1
1140 IF C = Ø THEN C = 1
1150 IF B > C GOTO 1100
1160 RETURN

```

Figure 19. Avalanche Detector, Quantized Output
Program Listing
(Sheet 3 of 3)

THESIS3 - THIS PROGRAM CALCULATES:
MO - THE NUMBER OF COUNTS PER SEGMENT USED TO DETERMINE
 A 1 OR 0 FOR THAT SEGMENT
 IF $N > MO$ DECIDE 1 FOR THAT SEGMENT
 IF $N < MO$ DECIDE 0 FOR THAT SEGMENT
CP1 - THE PROBABILITY OF DECIDING A 0 FOR A SEGMENT GIVEN
 MESSAGE 1 WAS SENT
CP0 - THE PROBABILITY OF DECIDING A 1 FOR A SEGMENT GIVEN
 MESSAGE 0 WAS SENT
L0 - THE NUMBER OF SEGMENTS WHERE A 1 WAS DECIDED
 REQUIRED TO MAKE THE FINAL DECISION THAT MESSAGE 1
 WAS SENT
 IF MORE THAN $L0$ OF THE J SEGMENTS ARE 1 THEN DECIDE
 MESSAGE 1 WAS SENT
 IF LESS THAN $L0$ OF THE J SEGMENTS ARE 1 THEN DECIDE
 MESSAGE 0 WAS SENT
P OF E - THE OVERALL SYSTEM PROBABILITY OF ERROR
 GIVEN THE INPUTS:
PR0 - THE PRIOR PROBABILITY OF MESSAGE 0
J - THE NUMBER OF SEGMENTS T IS DIVIDED INTO
M0 - THE AVERAGE COUNT FOR MESSAGE 0 BEING SENT
M1 - THE AVERAGE COUNT FOR MESSAGE 1 BEING SENT
M - THE AVERAGE GAIN OF THE AVALANCHE DETECTOR
K - THE HOLE IONIZATION COEFFICIENT TO ELECTRON
 IONIZATION COEFFICIENT RATIO

<u>J</u>	<u>PR0</u>	<u>PR1</u>	<u>M0</u>	<u>M1</u>	<u>K</u>	<u>M</u>
5	.5	.5	5	15	.5	10
<u>MO</u>	<u>CP0</u>	<u>CP1</u>	<u>L0</u>	<u>P OF E</u>		
4.38521	.475774	.149137	3.41895	.160942		

Figure 20. Avalanche Detector, Quantized Output Program
Sample Output

Appendix B

Data

Table II lists computed values of N_0 , $(1-p_0)$, $(1-p_1)$, L_0 , and $P(E)$ for several values of J , μ_0 , μ_1 and equiprobable priors, for the ideal unity gain detector. Table III lists computed values of \tilde{R}_0 given the crossover probabilities, $(1-p_0)$ and $(1-p_1)$, from Table II. Table IV lists computed values of N_0 , $(1-p_0)$, $(1-p_1)$, L_0 , and $P(E)$ for several values of J , μ_0 , μ_1 , and equiprobable priors, for the avalanche detector system. An avalanche detector with average gain of 10 and ionization coefficient ratio of .5 was used in calculating the values of Table IV. These values were used only to shorten calculation time and provide representative data. Table V lists computed values of \tilde{R}_0 given the crossover probabilities, $(1-p_0)$ and $(1-p_1)$, from Table IV.

TABLE II

Ideal Detector, Quantized Output
 $\Pr\{M_0\} = \Pr\{M_1\}$

<u>J</u>	<u>μ_0</u>	<u>μ_1</u>	<u>N_0</u>	<u>$(1-p_0)$</u>	<u>$(1-p_1)$</u>	<u>L_0</u>	<u>P(E)</u>
1	1	4	2.16	0.080	0.238	0.38	0.1592
2	1	4	1.08	0.090	0.406	0.60	0.1686
3	1	4	0.72	0.283	0.264	1.53	0.1837
4	1	4	0.54	0.221	0.368	1.67	0.1792
5	1	4	0.43	0.181	0.449	1.75	0.1777
10	1	4	0.22	0.095	0.670	1.94	0.1768
15	1	4	0.14	0.064	0.766	2.01	0.1750
20	1	4	0.11	0.049	0.819	2.05	0.1706
30	1	4	0.07	0.033	0.875	2.09	0.1665
40	1	4	0.05	0.025	0.905	2.11	0.1645
50	1	4	0.04	0.020	0.923	2.12	0.1634
60	1	4	0.04	0.017	0.936	2.13	0.1627
70	1	4	0.03	0.014	0.944	2.13	0.1622
80	1	4	0.03	0.012	0.951	2.14	0.1618
90	1	4	0.02	0.011	0.957	2.14	0.1615
100	1	4	0.02	0.010	0.961	2.14	0.1613
110	1	4	0.02	0.009	0.964	2.14	0.1611
120	1	4	0.02	0.008	0.967	2.14	0.1609
130	1	4	0.02	0.008	0.970	2.15	0.1608

TABLE II--CONTINUED

<u>J</u>	<u>μ_0</u>	<u>μ_1</u>	<u>N_0</u>	<u>$(1-p_0)$</u>	<u>$(1-p_1)$</u>	<u>L_0</u>	<u>P(E)</u>
1	1	5	2.49	0.080	0.124	0.46	0.1025
2	1	5	1.24	0.090	0.287	0.72	0.1274
3	1	5	0.83	0.283	0.189	1.68	0.1445
4	1	5	0.62	0.221	0.287	1.84	0.1440
5	1	5	0.50	0.181	0.368	1.95	0.1447
10	1	5	0.25	0.095	0.607	2.20	0.1201
15	1	5	0.17	0.064	0.717	2.29	0.1128
20	1	5	0.12	0.049	0.779	2.34	0.1097
30	1	5	0.08	0.033	0.846	2.38	0.1070
40	1	5	0.06	0.025	0.882	2.41	0.1058
50	1	5	0.05	0.020	0.905	2.42	0.1050
60	1	5	0.04	0.017	0.920	2.43	0.1046
70	1	5	0.04	0.014	0.931	2.44	0.1043
80	1	5	0.03	0.012	0.939	2.45	0.1040
90	1	5	0.03	0.011	0.946	2.45	0.1039
100	1	5	0.02	0.010	0.951	2.45	0.1037
110	1	5	0.02	0.009	0.956	2.46	0.1036
120	1	5	0.02	0.008	0.959	2.46	0.1035
130	1	5	0.02	0.008	0.962	2.46	0.1034

TABLE II--CONTINUED

<u>J</u>	<u>μ_0</u>	<u>μ_1</u>	<u>N_0</u>	<u>$(1-p_0)$</u>	<u>$(1-p_1)$</u>	<u>L_0</u>	<u>P(E)</u>
1	2	8	4.32	0.053	0.100	0.44	0.0761
2	2	8	2.16	0.080	0.238	0.75	0.1054
3	2	8	1.44	0.144	0.255	1.27	0.1091
4	2	8	1.08	0.090	0.406	1.20	0.1147
5	2	8	0.87	0.330	0.202	2.88	0.1319
10	2	8	0.43	0.181	0.449	3.51	0.0957
15	2	8	0.29	0.125	0.587	3.76	0.0910
20	2	8	0.22	0.095	0.670	3.89	0.0903
30	2	8	0.14	0.064	0.766	4.03	0.0886
40	2	8	0.11	0.049	0.818	4.10	0.0849
50	2	8	0.09	0.039	0.852	4.15	0.0828
60	2	8	0.07	0.033	0.875	4.18	0.0815
70	2	8	0.06	0.028	0.892	4.20	0.0807
80	2	8	0.05	0.025	0.905	4.21	0.0800
90	2	8	0.05	0.022	0.915	4.23	0.0796
100	2	8	0.04	0.020	0.923	4.24	0.0792
110	2	8	0.04	0.018	0.930	4.24	0.0789
120	2	8	0.04	0.017	0.936	4.25	0.0786
130	2	8	0.03	0.015	0.940	4.26	0.0784

TABLE II--CONTINUED

<u>J</u>	<u>μ_0</u>	<u>μ_1</u>	<u>N_0</u>	<u>$(1-p_0)$</u>	<u>$(1-p_1)$</u>	<u>L_0</u>	<u>P(E)</u>
1	2	10	4.97	0.053	0.029	0.54	0.0410
2	2	10	2.49	0.080	0.124	0.91	0.0848
3	2	10	1.66	0.144	0.155	1.48	0.0604
4	2	10	1.24	0.090	0.287	1.43	0.0588
5	2	10	0.99	0.330	0.135	3.12	0.0910
10	2	10	0.50	0.181	0.368	3.90	0.0624
15	2	10	0.33	0.125	0.513	4.22	0.0517
20	2	10	0.25	0.095	0.607	4.40	0.0466
30	2	10	0.17	0.064	0.717	4.58	0.0434
40	2	10	0.12	0.049	0.779	4.67	0.0423
50	2	10	0.10	0.039	0.819	4.73	0.0418
60	2	10	0.08	0.033	0.846	4.77	0.0416
70	2	10	0.07	0.028	0.867	4.80	0.0414
80	2	10	0.06	0.025	0.882	4.82	0.0413
90	2	10	0.06	0.022	0.895	4.84	0.0413
100	2	10	0.05	0.020	0.905	4.85	0.0412
110	2	10	0.05	0.018	0.913	4.86	0.0412
120	2	10	0.04	0.017	0.920	4.87	0.0411
130	2	10	0.04	0.015	0.926	4.88	0.0411

TABLE II--CONTINUED

<u>J</u>	<u>μ_0</u>	<u>μ_1</u>	<u>N_0</u>	<u>$(1-p_0)$</u>	<u>$(1-p_1)$</u>	<u>L_0</u>	<u>P(E)</u>
1	3	12	6.49	0.034	0.046	0.48	0.0397
2	3	12	3.25	0.066	0.151	0.83	0.0749
3	3	12	2.16	0.080	0.238	1.13	0.0807
4	3	12	1.62	0.173	0.199	1.93	0.0841
5	3	12	1.30	0.122	0.308	1.88	0.0748
10	3	12	0.65	0.259	0.301	4.76	0.0688
15	3	12	0.43	0.181	0.449	5.26	0.0580
20	3	12	0.32	0.139	0.549	5.54	0.0519
30	3	12	0.22	0.095	0.670	5.83	0.0495
40	3	12	0.16	0.072	0.741	5.99	0.0494
50	3	12	0.13	0.058	0.787	6.09	0.0469
60	3	12	0.11	0.049	0.819	6.15	0.0453
70	3	12	0.09	0.042	0.842	6.20	0.0443
80	3	12	0.08	0.037	0.861	6.24	0.0435
90	3	12	0.07	0.033	0.875	6.26	0.0430
100	3	12	0.06	0.030	0.887	6.29	0.0426
110	3	12	0.06	0.027	0.897	6.30	0.0423
120	3	12	0.05	0.025	0.905	6.32	0.0420
130	3	12	0.05	0.023	0.912	6.33	0.0418

TABLE II--CONTINUED

<u>J</u>	<u>μ_0</u>	<u>μ_1</u>	<u>N_0</u>	<u>$(1-p_0)$</u>	<u>$(1-p_1)$</u>	<u>L_0</u>	<u>$P(E)$</u>
1	3	15	7.46	0.012	0.018	0.48	0.0150
2	3	15	3.73	0.066	0.059	1.02	0.0596
3	3	15	2.49	0.080	0.125	1.37	0.0305
4	3	15	1.86	0.173	0.112	2.20	0.0412
5	3	15	1.49	0.122	0.199	2.20	0.0361
10	3	15	0.75	0.259	0.223	5.22	0.0371
15	3	15	0.50	0.181	0.368	5.86	0.0291
20	3	15	0.37	0.139	0.472	6.21	0.0245
30	3	15	0.25	0.095	0.607	6.60	0.0203
40	3	15	0.19	0.072	0.687	6.80	0.0195
50	3	15	0.15	0.058	0.741	6.92	0.0194
60	3	15	0.12	0.049	0.779	7.01	0.0193
70	3	15	0.11	0.042	0.807	7.07	0.0184
80	3	15	0.09	0.037	0.829	7.12	0.0178
90	3	15	0.08	0.033	0.846	7.15	0.0174
100	3	15	0.07	0.030	0.861	7.18	0.0171
110	3	15	0.07	0.027	0.873	7.21	0.0169
120	3	15	0.06	0.025	0.882	7.23	0.0167
130	3	15	0.06	0.023	0.891	7.25	0.0165

TABLE II--CONTINUED

<u>J</u>	<u>μ_0</u>	<u>μ_1</u>	<u>N_0</u>	<u>$(1-p_0)$</u>	<u>$(1-p_1)$</u>	<u>L_0</u>	<u>P(E)</u>
1	4	8	5.77	0.215	0.191	0.52	0.2031
2	4	8	2.89	0.323	0.238	1.10	0.2620
3	4	8	1.92	0.385	0.255	1.71	0.2461
4	4	8	1.44	0.264	0.406	1.69	0.2361
5	4	8	1.15	0.191	0.525	1.61	0.2325
10	4	8	0.58	0.330	0.449	4.38	0.2329
15	4	8	0.38	0.234	0.587	4.79	0.2249
20	4	8	0.29	0.181	0.670	5.01	0.2242
30	4	8	0.19	0.125	0.766	5.25	0.2136
40	4	8	0.14	0.095	0.819	5.37	0.2097
50	4	8	0.12	0.077	0.852	5.45	0.2078
60	4	8	0.10	0.064	0.875	5.50	0.2067
70	4	8	0.08	0.056	0.892	5.54	0.2060
80	4	8	0.07	0.049	0.904	5.57	0.2055
90	4	8	0.06	0.043	0.915	5.59	0.2052
100	4	8	0.06	0.039	0.923	5.61	0.2049
110	4	8	0.05	0.036	0.930	5.62	0.2047
120	4	8	0.05	0.033	0.936	5.63	0.2045
130	4	8	0.04	0.030	0.940	5.64	0.2044

TABLE II--CONTINUED

<u>J</u>	<u>μ_0</u>	<u>μ_1</u>	<u>N_0</u>	<u>$(1-p_0)$</u>	<u>$(1-p_1)$</u>	<u>L_0</u>	<u>$F(E)$</u>
1	4	12	7.28	0.051	0.090	0.45	0.0703
2	4	12	3.64	0.143	0.151	0.99	0.1441
3	4	12	2.43	0.151	0.238	1.32	0.1022
4	4	12	1.82	0.264	0.199	2.16	0.1193
5	4	12	1.46	0.191	0.308	2.14	0.1129
10	4	12	0.73	0.330	0.301	5.16	0.1126
15	4	12	0.49	0.234	0.449	5.76	0.0959
20	4	12	0.36	0.181	0.549	6.10	0.0916
30	4	12	0.24	0.125	0.670	6.46	0.0812
40	4	12	0.18	0.095	0.741	6.66	0.0786
50	4	12	0.15	0.077	0.787	6.78	0.0777
60	4	12	0.12	0.064	0.819	6.86	0.0774
70	4	12	0.10	0.056	0.842	6.92	0.0772
80	4	12	0.09	0.049	0.861	6.96	0.0772
90	4	12	0.08	0.043	0.875	6.99	0.0772
100	4	12	0.07	0.039	0.887	7.02	0.0765
110	4	12	0.07	0.036	0.897	7.05	0.0759
120	4	12	0.06	0.033	0.905	7.07	0.0753
130	4	12	0.06	0.030	0.912	7.08	0.0749

TABLE II--CONTINUED

<u>J</u>	<u>μ_0</u>	<u>μ_1</u>	<u>N_0</u>	<u>$(1-p_0)$</u>	<u>$(1-p_1)$</u>	<u>L_0</u>	<u>P(E)</u>
1	5	20	10.82	0.137	0.011	0.51	0.0123
2	5	20	5.41	0.042	0.067	0.92	0.0434
3	5	20	3.61	0.088	0.101	1.46	0.0252
4	5	20	2.71	0.132	0.125	2.02	0.0433
5	5	20	2.16	0.080	0.238	1.88	0.0339
10	5	20	1.08	0.090	0.406	2.99	0.0340
15	5	20	0.72	0.283	0.264	7.67	0.0300
20	5	20	0.54	0.221	0.368	8.33	0.0243
30	5	20	0.36	0.154	0.513	9.07	0.0207
40	5	20	0.27	0.118	0.607	9.47	0.0172
50	5	20	0.22	0.095	0.670	9.72	0.0163
60	5	20	0.18	0.080	0.716	9.90	0.0160
70	5	20	0.15	0.069	0.751	10.02	0.0158
80	5	20	0.14	0.061	0.779	10.12	0.0150
90	5	20	0.12	0.054	0.801	10.19	0.0145
100	5	20	0.11	0.049	0.819	10.25	0.0141
110	5	20	0.10	0.044	0.834	10.30	0.0138
120	5	20	0.09	0.041	0.846	10.35	0.0136
130	5	20	0.08	0.038	0.857	10.38	0.0134

TABLE II--CONTINUED

<u>J</u>	<u>ν_0</u>	<u>ν_1</u>	<u>N_0</u>	<u>$(1-p_0)$</u>	<u>$(1-p_1)$</u>	<u>L_0</u>	<u>P(E)</u>
1	5	25	12.43	0.002	0.003	0.48	0.0026
2	5	25	6.21	0.014	0.035	0.89	0.0147
3	5	25	4.14	0.028	0.082	1.24	0.0107
4	5	25	3.11	0.038	0.130	1.56	0.0082
5	5	25	2.49	0.080	0.125	2.28	0.0103
10	5	25	1.24	0.090	0.287	3.58	0.0085
15	5	25	0.83	0.283	0.189	8.39	0.0118
20	5	25	0.62	0.221	0.287	9.21	0.0088
30	5	25	0.41	0.154	0.435	10.15	0.0062
40	5	25	0.31	0.118	0.535	10.67	0.0048
50	5	25	0.25	0.095	0.607	10.99	0.0048
60	5	25	0.21	0.080	0.660	11.22	0.0040
70	5	25	0.18	0.069	0.700	11.38	0.0037
80	5	25	0.16	0.061	0.732	11.51	0.0035
90	5	25	0.14	0.054	0.757	11.60	0.0034
100	5	25	0.12	0.049	0.779	11.68	0.0034
110	5	25	0.11	0.044	0.797	11.75	0.0033
120	5	25	0.10	0.041	0.812	11.80	0.0033
130	5	25	0.10	0.038	0.825	11.85	0.0033

TABLE III
Symmetric Cutoff Rate for Ideal Detector

<u>J</u>	<u>μ_0</u>	<u>μ_1</u>	<u>$(1-p_0)$</u>	<u>$(1-p_1)$</u>	<u>\tilde{R}_0</u>	<u>P(E)*</u>
1	1	5	0.080	0.124	0.329	0.1025
2	1	5	0.090	0.287	0.336	0.1274
3	1	5	0.283	0.189	0.314	0.1445
4	1	5	0.221	0.287	0.347	0.1440
5	1	5	0.181	0.368	0.368	0.1447
10	1	5	0.095	0.607	0.408	0.1201
15	1	5	0.064	0.717	0.422	0.1128
20	1	5	0.049	0.779	0.428	0.1097
1	2	8	0.053	0.100	0.391	0.0761
2	2	8	0.080	0.238	0.404	0.1054
3	2	8	0.144	0.255	0.413	0.1091
4	2	8	0.090	0.406	0.419	0.1147
5	2	8	0.330	0.202	0.386	0.1319
10	2	8	0.181	0.449	0.468	0.0957
15	2	8	0.125	0.587	0.495	0.0910
20	2	8	0.095	0.670	0.508	0.0903
1	3	15	0.012	0.018	0.688	0.0150
2	3	15	0.066	0.059	0.697	0.0596
3	3	15	0.080	0.125	0.713	0.0305
4	3	15	0.173	0.112	0.695	0.0412
5	3	15	0.121	0.199	0.727	0.0361
10	3	15	0.259	0.223	0.726	0.0371
15	3	15	0.181	0.368	0.778	0.0291
20	3	15	0.139	0.472	0.802	0.0245

* P(E) from TABLE II

TABLE III--CONTINUED

<u>J</u>	<u>μ_0</u>	<u>μ_1</u>	<u>$(1-p_0)$</u>	<u>$(1-p_1)$</u>	<u>\tilde{R}_0</u>	<u>$P(E)^*$</u>
1	4	8	0.215	0.191	0.149	0.2031
2	4	8	0.323	0.238	0.147	0.2620
3	4	8	0.385	0.255	0.145	0.2461
4	4	8	0.264	0.406	0.160	0.2361
5	4	8	0.191	0.525	0.163	0.2325
10	4	8	0.330	0.449	0.172	0.2329
15	4	8	0.234	0.587	0.189	0.2249
20	4	8	0.181	0.670	0.198	0.2242
1	5	20	0.014	0.011	0.714	0.0123
2	5	20	0.042	0.067	0.732	0.0434
3	5	20	0.088	0.101	0.737	0.0252
4	5	20	0.132	0.125	0.738	0.0433
5	5	20	0.080	0.238	0.752	0.0339
10	5	20	0.090	0.406	0.769	0.0340
15	5	20	0.283	0.264	0.763	0.0300
20	5	20	0.221	0.368	0.800	0.0243

* $P(E)$ from TABLE II

TABLE IV

Avalanche Detector, Quantized Output
 $P\{M_0\} = P\{M_1\}$

<u>J</u>	<u>μ_0</u>	<u>μ_1</u>	<u>N_{0a}</u>	<u>$(1-p_0)$</u>	<u>$(1-p_1)$</u>	<u>L_0</u>	<u>$P(E)$</u>
1	5	20	82.36	0.193	0.091	0.59	0.1419
2	5	20	30.98	0.324	0.121	1.26	0.1663
3	5	20	16.16	0.376	0.141	1.93	0.1859
4	5	20	9.77	0.411	0.131	2.67	0.1388
5	5	20	6.39	0.414	0.130	3.35	0.1139
6	5	20	4.30	0.418	0.120	4.08	0.1029
7	5	20	3.13	0.407	0.123	4.70	0.0739
8	5	20	3.01	0.367	0.161	4.99	0.0771
9	5	20	5.62	0.283	0.286	4.48	0.0808
10	5	20	7.51	0.229	0.393	4.09	0.1052
1	5	25	101.87	0.141	0.059	0.59	0.0997
2	5	25	39.11	0.265	0.094	1.25	0.1252
3	5	25	20.84	0.333	0.106	1.95	0.1447
4	5	25	12.77	0.361	0.110	2.64	0.1003
5	5	25	8.50	0.370	0.112	3.32	0.0829
6	5	25	5.93	0.387	0.094	4.13	0.0692
7	5	25	4.18	0.372	0.103	4.71	0.0497
8	5	25	3.17	0.367	0.101	5.38	0.0357
9	5	25	2.65	0.374	0.090	6.17	0.0289
10	5	25	4.87	0.280	0.205	5.46	0.0352
11	5	25	6.68	0.224	0.315	4.91	0.0530
12	5	25	8.09	0.187	0.408	4.49	0.0605

TABLE IV--CONTINUED

<u>J</u>	<u>μ_0</u>	<u>μ_1</u>	<u>N_{0a}</u>	<u>$(1-p_0)$</u>	<u>$(1-p_1)$</u>	<u>L_0</u>	<u>$P(E)$</u>
1	6	12	57.41	0.375	0.229	0.58	0.3019
2	6	12	20.68	0.476	0.240	1.25	0.3244
3	6	12	10.51	0.528	0.228	1.97	0.3369
4	6	12	6.16	0.541	0.220	2.67	0.2943
5	6	12	3.81	0.583	0.173	3.58	0.2588
6	6	12	2.76	0.572	0.180	4.24	0.2434
7	6	12	5.26	0.396	0.377	3.57	0.2643
8	6	12	7.92	0.316	0.488	3.29	0.2812
1	6	18	80.96	0.247	0.131	0.58	0.1895
2	6	18	30.55	0.362	0.166	1.23	0.2181
3	6	18	16.04	0.420	0.182	1.90	0.2338
4	6	18	9.13	0.462	0.165	2.67	0.1937
5	6	18	6.39	0.469	0.161	3.36	0.1685
6	6	18	4.33	0.476	0.149	4.10	0.1549
7	6	18	3.15	0.465	0.153	4.74	0.1254
8	6	18	2.88	0.470	0.144	5.48	0.1020
9	6	18	5.52	0.327	0.323	4.52	0.1323
10	6	18	7.51	0.266	0.428	4.13	0.1577

TABLE IV--CONTINUED

<u>J</u>	<u>μ_0</u>	<u>μ_1</u>	<u>N_{0a}</u>	<u>$(1-p_0)$</u>	<u>$(1-p_1)$</u>	<u>L_0</u>	<u>$P(E)$</u>
1	8	32	150.36	0.125	0.066	0.56	0.0957
2	8	32	61.39	0.231	0.104	1.19	0.1254
3	8	32	34.12	0.306	0.125	1.86	0.1331
4	8	32	21.83	0.359	0.130	2.57	0.1100
5	8	32	15.09	0.379	0.143	3.21	0.1120
6	8	32	10.98	0.410	0.129	4.01	0.1104
7	8	32	8.27	0.406	0.138	4.62	0.0812
8	8	32	6.39	0.414	0.130	5.36	0.0668
9	8	32	4.98	0.438	0.104	6.32	0.0505
10	8	32	3.90	0.443	0.095	7.12	0.0435
11	8	32	3.21	0.413	0.119	7.46	0.0342
12	8	32	2.79	0.431	0.100	8.43	0.0258
13	8	32	3.39	0.363	0.166	8.03	0.0330
14	8	32	5.05	0.289	0.276	7.10	0.0441
15	8	32	6.39	0.256	0.337	6.81	0.0484
16	8	32	7.51	0.229	0.393	6.54	0.0521
17	8	32	8.48	0.207	0.442	6.30	0.0588

TABLE IV--CONTINUED

<u>J</u>	<u>μ_0</u>	<u>μ_1</u>	<u>N_{0a}</u>	<u>$(1-p_0)$</u>	<u>$(1-p_1)$</u>	<u>L_0</u>	<u>$P(E)$</u>
1	8	40	185.04	0.075	0.040	0.55	0.0575
2	8	40	76.23	0.177	0.072	1.19	0.0851
3	8	40	43.20	0.253	0.092	1.86	0.0918
4	8	40	27.81	0.307	0.099	2.57	0.0705
5	8	40	19.44	0.334	0.110	3.24	0.0712
6	8	40	14.31	0.350	0.116	3.90	0.0707
7	8	40	10.88	0.370	0.108	4.67	0.0507
8	8	40	8.50	0.370	0.112	5.31	0.0424
9	8	40	6.76	0.380	0.102	6.10	0.0372
10	8	40	5.43	0.376	0.104	6.74	0.0268
11	8	40	4.40	0.377	0.099	7.47	0.0189
12	8	40	3.82	0.386	0.086	8.34	0.0136
13	8	40	3.10	0.363	0.105	8.67	0.0120
14	8	40	2.75	0.383	0.084	9.73	0.0084
15	8	40	3.42	0.324	0.142	9.23	0.0099
16	8	40	4.87	0.280	0.205	8.74	0.0122
17	8	40	6.06	0.231	0.303	7.78	0.0196
18	8	40	7.07	0.208	0.356	7.45	0.0223
19	8	40	7.93	0.198	0.375	7.57	0.0215

TABLE IV--CONTINUED

<u>J</u>	<u>μ_0</u>	<u>μ_1</u>	<u>N_{0a}</u>	<u>$(1-p_0)$</u>	<u>$(1-p_1)$</u>	<u>L_0</u>	<u>$P(E)$</u>
1	10	30	154.88	0.179	0.104	0.56	0.1414
2	10	30	63.59	0.273	0.143	1.17	0.1703
3	10	30	35.79	0.345	0.160	1.84	0.1721
4	10	30	23.03	0.388	0.177	2.49	0.1564
5	10	30	16.04	0.420	0.182	3.17	0.1644
6	10	30	11.74	0.452	0.168	3.96	0.1614
7	10	30	8.91	0.471	0.158	4.73	0.1329
8	10	30	6.93	0.482	0.149	5.49	0.1128
9	10	30	5.46	0.475	0.153	6.12	0.1081
10	10	30	4.33	0.476	0.149	6.84	0.0920
11	10	30	3.60	0.485	0.136	7.67	0.0731
12	10	30	3.03	0.456	0.161	7.99	0.0759
13	10	30	2.67	0.478	0.137	9.02	0.0619
14	10	30	4.04	0.372	0.257	7.89	0.0741
15	10	30	5.52	0.327	0.323	7.53	0.0772
16	10	30	6.77	0.291	0.382	7.21	0.0873
17	10	30	7.85	0.262	0.435	6.92	0.0975
18	10	30	8.79	0.237	0.482	6.67	0.1009

TABLE IV--CONTINUED

<u>J</u>	<u>μ_0</u>	<u>μ_1</u>	<u>N_{0a}</u>	<u>$(1-p_0)$</u>	<u>$(1-p_1)$</u>	<u>L_0</u>	<u>$P(E)$</u>
1	10	40	195.01	0.102	0.052	0.56	0.0769
2	10	40	82.36	0.193	0.091	1.17	0.1053
3	10	40	47.26	0.266	0.113	1.83	0.1047
4	10	40	30.98	0.324	0.121	2.53	0.0887
5	10	40	21.83	0.359	0.130	3.22	0.0941
6	10	40	16.16	0.376	0.141	3.86	0.0939
7	10	40	12.41	0.394	0.139	4.57	0.0759
8	10	40	9.77	0.411	0.131	5.34	0.0662
9	10	40	7.84	0.420	0.125	6.09	0.0624
10	10	40	6.39	0.414	0.130	6.70	0.0487
11	10	40	5.23	0.413	0.129	7.37	0.0394
12	10	40	4.30	0.418	0.120	8.15	0.0338
13	10	40	3.80	0.430	0.105	9.08	0.0268
14	10	40	3.13	0.407	0.123	9.40	0.0209
15	10	40	2.79	0.431	0.100	10.54	0.0151
16	10	40	3.01	0.367	0.161	9.98	0.0203
17	10	40	4.43	0.320	0.225	9.44	0.0212
18	10	40	5.62	0.283	0.286	8.97	0.0284
19	10	40	6.63	0.253	0.342	8.55	0.0302
20	10	40	7.51	0.229	0.393	8.18	0.0366

TABLE V

Symmetric Cutoff Rate for Avalanche Detector
 $P\{M_0\} = P\{M_1\}$

<u>J</u>	<u>μ_0</u>	<u>μ_1</u>	<u>$(1-p_0)$</u>	<u>$(1-p_1)$</u>	<u>\tilde{R}_0</u>	<u>P(E)*</u>
1	5	20	0.193	0.091	0.243	0.1419
2	5	20	0.324	0.121	0.259	0.1663
3	5	20	0.376	0.141	0.280	0.1859
4	5	20	0.411	0.131	0.333	0.1388
5	5	20	0.414	0.130	0.399	0.1139
6	5	20	0.418	0.120	0.478	0.1029
7	5	20	0.407	0.123	0.546	0.0739
8	5	20	0.367	0.161	0.578	0.0771
9	5	20	0.283	0.286	0.518	0.0808
10	5	20	0.229	0.393	0.464	0.1052
1	5	25	0.141	0.059	0.332	0.0997
2	5	25	0.265	0.094	0.352	0.1252
3	5	25	0.333	0.106	0.382	0.1447
4	5	25	0.361	0.110	0.435	0.1003
5	5	25	0.370	0.112	0.499	0.0829
6	5	25	0.387	0.094	0.586	0.0692
7	5	25	0.372	0.103	0.648	0.0497
8	5	25	0.367	0.101	0.714	0.0357
9	5	25	0.374	0.090	0.775	0.0289
10	5	25	0.280	0.205	0.724	0.0352
11	5	25	0.224	0.315	0.661	0.0530
12	5	25	0.187	0.408	0.603	0.0605

* P(E) from TABLE IV

AD-A124 767

INVESTIGATION OF BINARY ERROR PROBABILITY FOR AN
INTEGRATE-AND-DUMP RECEI... (U) AIR FORCE INST OF TECH
WRIGHT-PATTERSON AFB OH SCHOOL OF ENGI... B T MELUSEN
DEC 82 AFIT/GE/EE/82D-49 F/G 1772

2/2

UNCLASSIFIED

NL

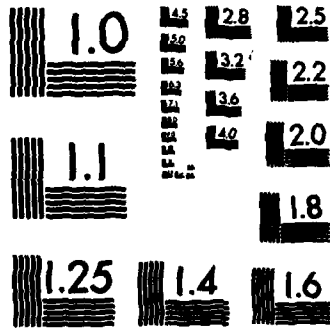


END

FORMED

BY

DTIC



MICROCOPY RESOLUTION TEST CHART
NATIONAL BUREAU OF STANDARDS-1963-A

TABLE V

Symmetric Cutoff Rate for Avalanche Detector
 $P\{M_0\} = P\{M_1\}$

<u>J</u>	<u>μ_0</u>	<u>μ_1</u>	<u>$(1-p_0)$</u>	<u>$(1-p_1)$</u>	<u>\tilde{R}_0</u>	<u>$P(E)^*$</u>
1	5	20	0.193	0.091	0.243	0.1419
2	5	20	0.324	0.121	0.259	0.1663
3	5	20	0.376	0.141	0.280	0.1859
4	5	20	0.411	0.131	0.333	0.1388
5	5	20	0.414	0.130	0.399	0.1139
6	5	20	0.418	0.120	0.478	0.1029
7	5	20	0.407	0.123	0.546	0.0739
8	5	20	0.367	0.161	0.578	0.0771
9	5	20	0.283	0.286	0.518	0.0808
10	5	20	0.229	0.393	0.464	0.1052
1	5	25	0.141	0.059	0.332	0.0997
2	5	25	0.265	0.094	0.352	0.1252
3	5	25	0.333	0.106	0.382	0.1447
4	5	25	0.361	0.110	0.435	0.1003
5	5	25	0.370	0.112	0.499	0.0829
6	5	25	0.387	0.094	0.586	0.0692
7	5	25	0.372	0.103	0.648	0.0497
8	5	25	0.367	0.101	0.714	0.0357
9	5	25	0.374	0.090	0.775	0.0289
10	5	25	0.280	0.205	0.724	0.0352
11	5	25	0.224	0.315	0.661	0.0530
12	5	25	0.187	0.408	0.603	0.0605

* $P(E)$ from TABLE IV

TABLE V--CONTINUED

<u>J</u>	<u>μ_0</u>	<u>μ_1</u>	<u>$(1-p_0)$</u>	<u>$(1-p_1)$</u>	<u>\tilde{R}_0</u>	<u>P(E)*</u>
1	6	12	0.375	0.229	0.062	0.3019
2	6	12	0.476	0.240	0.063	0.3244
3	6	12	0.528	0.228	0.072	0.3369
4	6	12	0.541	0.220	0.093	0.2943
5	6	12	0.583	0.173	0.130	0.2588
6	6	12	0.572	0.180	0.156	0.2434
7	6	12	0.396	0.377	0.127	0.2643
8	6	12	0.316	0.488	0.112	0.2812
1	6	18	0.247	0.131	0.170	0.1895
2	6	18	0.362	0.166	0.180	0.2181
3	6	18	0.420	0.182	0.188	0.2338
4	6	18	0.462	0.165	0.223	0.1937
5	6	18	0.469	0.161	0.271	0.1685
6	6	18	0.476	0.149	0.331	0.1549
7	6	18	0.465	0.153	0.385	0.1254
8	6	18	0.470	0.144	0.442	0.1020
9	6	18	0.327	0.323	0.363	0.1323
10	6	18	0.266	0.428	0.320	0.1577

* P(E) from TABLE IV

TABLE V--CONTINUED

<u>J</u>	<u>μ_0</u>	<u>μ_1</u>	<u>$(1-p_0)$</u>	<u>$(1-p_1)$</u>	<u>\tilde{R}_0</u>	<u>$P(E)^*$</u>
1	8	32	0.125	0.066	0.338	0.0957
2	8	32	0.231	0.104	0.373	0.1254
3	8	32	0.306	0.125	0.381	0.1331
4	8	32	0.359	0.130	0.400	0.1100
5	8	32	0.379	0.143	0.422	0.1120
6	8	32	0.410	0.129	0.470	0.1104
7	8	32	0.406	0.138	0.513	0.0812
8	8	32	0.414	0.130	0.570	0.0668
9	8	32	0.438	0.104	0.643	0.0505
10	8	32	0.443	0.095	0.702	0.0435
11	8	32	0.413	0.119	0.726	0.0342
12	8	32	0.431	0.100	0.777	0.0258
13	8	32	0.363	0.166	0.764	0.0330
14	8	32	0.289	0.276	0.701	0.0441
15	8	32	0.256	0.337	0.673	0.0484
16	8	32	0.229	0.393	0.645	0.0521
17	8	32	0.207	0.442	0.620	0.0588

* $P(E)$ from TABLE IV

TABLE V--CONTINUED

<u>J</u>	<u>μ_0</u>	<u>μ_1</u>	<u>$(1-p_0)$</u>	<u>$(1-p_1)$</u>	<u>\tilde{R}_0</u>	<u>$P(E)^*$</u>
1	8	40	0.075	0.040	0.453	0.0575
2	8	40	0.177	0.072	0.493	0.0851
3	8	40	0.253	0.092	0.507	0.0918
4	8	40	0.307	0.099	0.530	0.0705
5	8	40	0.334	0.110	0.555	0.0712
6	8	40	0.350	0.116	0.590	0.0707
7	8	40	0.370	0.108	0.640	0.0507
8	8	40	0.370	0.112	0.684	0.0424
9	8	40	0.380	0.102	0.739	0.0372
10	8	40	0.376	0.104	0.780	0.0268
11	8	40	0.377	0.099	0.823	0.0189
12	8	40	0.386	0.086	0.866	0.0136
13	8	40	0.363	0.105	0.880	0.0120
14	8	40	0.383	0.084	0.913	0.0084
15	8	40	0.324	0.142	0.903	0.0099
16	8	40	0.280	0.205	0.885	0.0122
17	8	40	0.231	0.303	0.833	0.0196
18	8	40	0.208	0.356	0.809	0.0223
19	8	40	0.198	0.375	0.817	0.0215

* P(E) from TABLE IV

TABLE V--CONTINUED

<u>J</u>	<u>μ_0</u>	<u>μ_1</u>	<u>$(1-p_0)$</u>	<u>$(1-p_1)$</u>	<u>\tilde{R}_0</u>	<u>P(E)*</u>
1	10	30	0.179	0.104	0.241	0.1414
2	10	30	0.273	0.143	0.278	0.1703
3	10	30	0.345	0.160	0.286	0.1721
4	10	30	0.388	0.177	0.287	0.1564
5	10	30	0.420	0.182	0.297	0.1644
6	10	30	0.452	0.168	0.328	0.1614
7	10	30	0.471	0.158	0.365	0.1329
8	10	30	0.482	0.149	0.410	0.1128
9	10	30	0.475	0.153	0.452	0.1081
10	10	30	0.476	0.149	0.499	0.0920
11	10	30	0.485	0.136	0.553	0.0731
12	10	30	0.456	0.161	0.576	0.0759
13	10	30	0.478	0.137	0.630	0.0619
14	10	30	0.372	0.257	0.569	0.0741
15	10	30	0.327	0.323	0.540	0.0772
16	10	30	0.291	0.382	0.514	0.0873
17	10	30	0.262	0.435	0.486	0.0975
18	10	30	0.237	0.482	0.462	0.1009

* P(E) from TABLE IV

TABLE V--CONTINUED

<u>J</u>	<u>μ_0</u>	<u>μ_1</u>	<u>$(1-p_0)$</u>	<u>$(1-p_1)$</u>	<u>\bar{R}_0</u>	<u>P(E)*</u>
1	10	40	0.102	0.052	0.389	0.0769
2	10	40	0.193	0.091	0.438	0.1053
3	10	40	0.266	0.113	0.451	0.1047
4	10	40	0.324	0.121	0.463	0.0887
5	10	40	0.359	0.130	0.477	0.0941
6	10	40	0.376	0.141	0.495	0.0939
7	10	40	0.394	0.139	0.530	0.0759
8	10	40	0.411	0.131	0.573	0.0662
9	10	40	0.420	0.125	0.619	0.0624
10	10	40	0.414	0.130	0.659	0.0487
11	10	40	0.413	0.129	0.701	0.0394
12	10	40	0.418	0.120	0.749	0.0338
13	10	40	0.430	0.105	0.796	0.0268
14	10	40	0.407	0.123	0.815	0.0209
15	10	40	0.431	0.100	0.854	0.0151
16	10	40	0.367	0.161	0.841	0.0203
17	10	40	0.320	0.225	0.816	0.0212
18	10	40	0.283	0.286	0.789	0.0284
19	10	40	0.253	0.342	0.762	0.0302
20	10	40	0.229	0.393	0.734	0.0366

* P(E) from TABLE IV

Vita

Bruce T. Melusen was born on 16 April 1951 in New York City, New York. He graduated from high school in West Islip, New York in 1969 and attended Rensselaer Polytechnic Institute in Troy, New York from where he received the degree of Bachelor of Science in Electrical Engineering in May 1973. He attended Officer Training School at Lackland AFB, Texas beginning February 1975 and was commissioned in May 1975. He was then assigned to the 90th Strategic Missile Wing, Technical Engineering Division, F. E. Warren AFB, Wyoming as an electrical engineer. During this assignment, he attended the University of Wyoming and was awarded a Masters Degree in Business Administration in December 1978. In 1979, he was assigned to the Armament Division, Eglin AFB, Florida where he worked as an electrical engineer in the Precision Guided Munitions Systems Program Office on the GBU-15 program. He entered the School of Engineering, Air Force Institute of Technology, in June 1981.

Permanent Address: 754 Tanglewood Road
West Islip, New York 11795

UNCLASSIFIED

SECURITY CLASSIFICATION OF THIS PAGE (When Data Entered)

REPORT DOCUMENTATION PAGE		READ INSTRUCTIONS BEFORE COMPLETING FORM
1. REPORT NUMBER AFIT/GE/EE/82D-49	2. GOVT ACCESSION NO. A0A124767	3. RECIPIENT'S CATALOG NUMBER
4. TITLE (and Subtitle) INVESTIGATION OF BINARY ERROR PROBABILITY FOR AN INTEGRATE-AND-DUMP RECEIVER AS OUTPUT QUANTIZATION INCREASES		5. TYPE OF REPORT & PERIOD COVERED MS THESIS
7. AUTHOR(s) Bruce T. Melusen Captain USAF		6. PERFORMING ORG. REPORT NUMBER
9. PERFORMING ORGANIZATION NAME AND ADDRESS Air Force Institute of Technology (AFIT/EN) Wright-Patterson AFB, Ohio 45433		8. CONTRACT OR GRANT NUMBER(s)
11. CONTROLLING OFFICE NAME AND ADDRESS		10. PROGRAM ELEMENT, PROJECT, TASK AREA & WORK UNIT NUMBERS
14. MONITORING AGENCY NAME & ADDRESS (if different from Controlling Office)		12. REPORT DATE December 1982
		13. NUMBER OF PAGES 90
		15. SECURITY CLASS. (of this report) Unclassified
		15a. DECLASSIFICATION/DOWNGRADING SCHEDULE
16. DISTRIBUTION STATEMENT (of this Report) Approved for public release; distribution unlimited.		
17. DISTRIBUTION STATEMENT (of the abstract entered in Block 20, if different from Report)		
18. SUPPLEMENTARY NOTES Approved for public release, IAW AFR 190-17 <i>Lynn E. Wolaver</i> LYNN E. WOLAVER Dean for Research and Professional Development Air Force Institute of Technology (ATC) Wright-Patterson AFB OH 45433		
19. KEY WORDS (Continue on reverse side if necessary and identify by block number) Direct Detection Error Probability Quantized Output		
20. ABSTRACT (Continue on reverse side if necessary and identify by block number) The binary error probability for integrate-and-dump receivers is developed. The combination of the optical modulator, optical channel, and optical detector is characterized as a discrete memoryless channel (DMC). Maximum a posteriori (MAP) decision criteria are developed to enable optimal post-detection processing. The effect of quantizing the output is addressed for both ideal unity gain detector and avalanche detector optical systems. Multilevel Amplitude Keying is used to calculate specific		

DD FORM 1 JAN 73 1473

EDITION OF 1 NOV 65 IS OBSOLETE

UNCLASSIFIED

SECURITY CLASSIFICATION OF THIS PAGE (When Data Entered)

UNCLASSIFIED

SECURITY CLASSIFICATION OF THIS PAGE(When Data Entered)

BLOCK 20. CONTINUED

probability of error values, and the channel cutoff rate is used to investigate probability of error bounds.

SECURITY CLASSIFICATION OF THIS PAGE(When Data Entered)